

11-14-2016

Expansion of the Performance Capabilities of the USF Inhalation Challenge Chamber

Laura Riley

University of South Florida, laura.f.riley@gmail.com

Follow this and additional works at: <http://scholarcommons.usf.edu/etd>



Part of the [Environmental Health and Protection Commons](#), and the [Public Health Commons](#)

Scholar Commons Citation

Riley, Laura, "Expansion of the Performance Capabilities of the USF Inhalation Challenge Chamber" (2016). *Graduate Theses and Dissertations*.

<http://scholarcommons.usf.edu/etd/6575>

This Dissertation is brought to you for free and open access by the Graduate School at Scholar Commons. It has been accepted for inclusion in Graduate Theses and Dissertations by an authorized administrator of Scholar Commons. For more information, please contact scholarcommons@usf.edu.

Expansion of the Performance Capabilities of the USF Inhalation Challenge Chamber

by

Laura Farina Riley

A dissertation submitted in partial fulfillment
of the requirements for a degree of
Doctor of Philosophy
Department of Environmental and Occupational Health
College of Public Health
University of South Florida

Major Professor: Yehia Y. Hammad, Sc.D.
Thomas J. Mason, Ph.D.
Steven P. Mlynarek, Ph.D.
Luis F. Pieretti, Ph.D.
Rene R. Salazar, Ph.D.

Date of Approval:
October 21, 2016

Keywords: inhalation challenge, aerosol generation, particulate matter, aerosol, thoracic-fraction

Copyright © 2016, Laura Farina Riley

Dedication

I would like to dedicate this dissertation to my ever-supportive and loving husband, Mike. His handyman prowess was instrumental in some of the chamber reconfigurations, and his positive and optimistic outlook on the whole process helped me get through some long days. I also want to include our children, Everett and Allison, in this dedication. They are the reason I did not give up and I am so glad they will grow up knowing that you can accomplish anything with the love and support of family.

Acknowledgments

I would like to express my sincerest thanks to Dr. Yehia Hammad for his insight, direction, and patience throughout my doctoral academic career. I am fortunate to have had the pleasure of working with such a renowned figure in the field of industrial hygiene.

I would also like to thank Drs. Thomas Mason, Steven Mlynarek, Luis Pieretti, and Rene Salazar for their thoughtful contributions and feedback throughout the course of this research.

This research would not have been possible without funding from the National Institute for Occupational Safety and Health under training grant T42-OH008438. I earnestly thank NIOSH for their continued support of our program and my research.

Table of Contents

List of Acronyms, Abbreviations, and Symbols	iii
List of Tables	v
List of Figures	vi
List of Equations	vii
Abstract	viii
Introduction	1
Purpose of the Study	1
Research Hypotheses	1
Aerosols: Background	2
Types of Exposure Chambers	2
Literature Review	6
Health Effects of Air Pollution	6
Other Exposure Chamber Studies	10
Experimental Methods	21
Chamber Specifications	21
Exposure Chamber Components	22
Characteristics and Generation of Experimental Aerosol	23
Aerosol Measurement	26
System Configurations	28
Step 1: Removal of the vertical elutriator & elimination of 6 ft of PVC pipe	28
Step 2: Mixing chamber positioned horizontally	29
Step 3: Placing mixing chamber directly over dust generator/RPM Reduction	29
Step 4: Additional clean air	31
Step 5: Increasing glass beads to a nominal size of 7-15 μm	33
Step 6: Slanted PVC configuration	34
Step 7: Elimination of Tygon tubing on WDF/Wider PVC opening	34
Step 8: Heated glass beads	36
Step 9: Increasing glass beads to a nominal size of 25 μm	36
Analysis of Data	36
Results and Discussion	37
Section A: Particle Size Distributions	37
Section B: Distribution of Concentration across the Exposure Chamber	40
Conclusions	47

Research Hypotheses	47
Particle Size Distribution: Major Findings	47
Evenness of Concentration: Major Findings.....	48
Study Strengths and Limitations	48
Public Health Implications and Future Directions	49
References.....	51
Appendices.....	56
Appendix A: Rotameter Calibration	57
Appendix B: Critical Orifice Calibrations	58
Appendix C: Determination of Size Distribution of Glass Beads by Light Microscopy	59
Appendix D: Mannequin Measurements	60
Appendix E: Particle Size Distribution for Each Reconfiguration Step	61
Appendix F: An Example of a DPlot graph as Determined by Impactor	62
Appendix G: MSDS for Soda Lime Glass Beads	63
Appendix H: TEOM Data vs Gravimetric Data for Average Particle Concentration.....	64
Appendix I: Copyright Clearance - John Wiley & Sons	65

List of Acronyms, Abbreviations, and Symbols

ACGIH	American Conference of Governmental Industrial Hygienists
ANOVA	Analysis of Variance
C	Concentration
Cfm	Cubic Feet per Minute
COPD	Chronic Obstructive Pulmonary Disease
CV	Coefficient of Variation
d_{ae}	Aerodynamic Diameter
EPA	Environmental Protection Agency
ETS	Environmental Tobacco Smoke
G	Generation Rate of Challenge Agent
GSD	Geometric Standard Deviation
HEC	Human Exposure Chamber
HEPA	High Efficiency Particulate Air
K	Mixing Factor
L	Liter
L/min	Liters per minute
m^3	Cubic meter
μg	Microgram
$\mu\text{m}/\text{um}$	Micrometer
mg	Milligram
min	Minute
MMD	Mass Median Diameter
NAAQS	National Ambient Air Quality Standards
ng	Nanogram
PM	Particulate Matter
PVC	Polyvinyl Chloride

Q	Volumetric Flow Rate (L/min)
Δt	Change in Time
TEOM	Tapered Element Oscillating Microbalance
V	Volume (liters)
WHO	World Health Organization
WDF	Wright Dust Feed

List of Tables

Table 1: ACGIH Inhalable Fraction6

Table 2: ACGIH Thoracic Fraction7

Table 3: ACGIH Respirable Fraction7

Table 4: EPA National Ambient Air Quality Standards for Particle Pollution9

Table 5: Mass Median Diameter (MMD) Obtained for each Chamber Configuration Step38

Table 6: Tests for Normality for each Configuration Step39

Table 7: Statistical Comparison Between Each Configuration – Independent Samples t-test40

Table 8: Filter Concentrations Normalized to the Mean42

Table 9: Test for Normality: Evenness of Concentration44

Table 10: Statistical Comparison of Open Face Cassette Patterns44

Table 11: Average Dust Concentrations Corresponding to Chamber Configurations,
Obtained by Gravimetric Analysis.....46

List of Figures

Figure 1: Diagram of Inhalation System.....	22
Figure 2: Photomicrograph of soda lime glass beads between 1 μm and 1 mm (2014).....	24
Figure 3: Diagram of Wright Dust Feed Mechanism (Hinds, 1999).....	25
Figure 4: T-Shape Configuration	29
Figure 5: New End Cap with Second Nozzle for Additional Nitrogen, Side View.....	30
Figure 6: New End Cap with Second Nozzle for Additional Nitrogen - Underside.....	30
Figure 7: End Cap Reconfigured with Four Perimeter Nozzles for Clean Air.....	31
Figure 8: End Cap Reconfigured with Four Perimeter Nozzles for Clean Air Inside View	32
Figure 9: Shortened Tubing from Wright Dust Feed to End Cap.....	32
Figure 10: Mannequin Inside Chamber	33
Figure 11: Slanted Junction Where Clean Air Meets Dust-Laden Air	34
Figure 12: WDF Feeding Directly into End Cap	35
Figure 13: WDF Feeding Directly into End Cap - Enlarged Image	35
Figure 14: Average Particle Diameter Obtained for Each Step.....	38
Figure 15: Plan view of Chamber with Numbered Cassette Locations	41
Figure 16: Plan View of Chamber Showing Groups A and B.....	41
Figure 17: Plan View of Chamber Showing Groups C, D, and E	42
Figure 18: Chamber Diagram Showing Normalized Filter Concentrations	43
Figure 19: Comparison Quantile Plots for Groups A and B.....	45

List of Equations

Equation 1	3
Equation 2	4
Equation 3	4
Equation 4	5

Abstract

The purpose of this research was to evaluate the capability and performance of the University of South Florida's (USF) Human Exposure Chamber (HEC) using aerosols in the thoracic range. The goals of this research were two-fold: to obtain an average particle size of 10 μm (thoracic-size range) inside the chamber during dust production and to test for evenness of dust concentration within the chamber. The USF HEC can be used for studies using gases and/or particulates. The chamber measurements are 4.16 ft x 2.67 ft x 6.75 ft, for a total volume of 75 ft^3 or 2.13 m^3 . This research has public health significance since outdoor air pollution is found most commonly in the thoracic size range; future studies with the HEC could focus on the impact of outdoor air pollution on human subjects under various exposure conditions, and various particle size ranges. Soda lime glass beads were used in this study due to their uniformity in shape and size. A Wright Dust Feeder (WDF) was used to generate the glass beads aerosol in the chamber. Nitrogen gas and HEPA-filtered fresh air were used to transport the aerosol through the system and into the chamber. A total of nine different chamber configurations were made in order to increase the average particle size closer to the goal of 10 μm . Chamber reconfiguration provided statistically significant effect on increasing particle size with the exception of two intermediate settings. It was concluded that aerosol distribution within the chamber was even during operation of the chamber, and modification steps utilized in the study provided size distribution within +/- 6% of the target particle size.

Introduction

Purpose of the Study

The purpose of this study was to enhance the capabilities of a whole-body human exposure chamber (HEC) to generate consistently an even distribution of particles in the thoracic size range. The chamber is located in the Breath Laboratory of the Sunshine Education and Research Center at the University of South Florida's (USF's) College of Public Health. Previous work has been conducted with this chamber to generate particles in the respirable range.

Research Hypotheses

For average particle size distribution at each reconfiguration step:

H_0 : There is no statistical difference between the thoracic-fraction size distribution obtained with each configuration of the aerosol generation system.

H_1 : There are statistical differences between the thoracic-fraction size distribution obtained with each configuration of the aerosol generation system.

For evenness of concentration across the chamber:

H_0 : There is no statistical difference between total aerosol concentrations obtained by aerosol sampling for each cassette within the chamber.

H_1 : There are statistical differences between total aerosol concentrations obtained by aerosol sampling for each cassette within the chamber.

Aerosols: Background

Aerosols are solid or liquid particles suspended in gas, and the term 'aerosol' includes both the particles and the gas in which they are suspended. The particle size range of aerosols can be anywhere from 0.002 to greater than 1000 micrometers (μm) (Hinds, 1999). A particle's size can be measured physically or dynamically (McClellan & Henderson, 1995). Physical particle size relates to a particle's geometry whereas dynamic size includes aerodynamic and mobility diameters (McClellan & Henderson, 1995). A particle's aerodynamic diameter (d_{ae}) is the diameter at which a spherical particle with a density of 1 g/cm^3 has the same settling velocity as the particle in question (Hinds, 1999). The mobility diameter of a particle is the diameter at which a spherical particle has the same dynamic mobility as the particle in question. This dynamic mobility can be defined as particle velocity divided by resistance force (McClellan & Henderson, 1995).

Types of Exposure Chambers

There are two categories of exposure chambers: whole body and nose only. Nose only is preferred because it prevents exposure through the skin and ensures that dust exposure is only through inhalation. In this study we are concerned with whole body exposure, and will therefore be using a human exposure chamber. The chambers described below are also human exposure chambers.

Inhalation challenge human exposure chambers can be divided into three types based on the method of delivery and particle size of the delivered agent. Static exposure systems utilize a finite amount of the agent in the chamber that is added at the beginning of the test. This can

result in a depletion of oxygen concentration, increase in the temperature in the chamber, and change in the concentration of the agent. Recirculating exposure systems have a closed-loop agent delivery. The recirculation does not remove water (H₂O) or carbon dioxide (CO₂), and also depletes the concentration of the aerosol; after exposure begins, no further aerosol is added, therefore a steady concentration within the chamber cannot be maintained (McClellan & Henderson, 1995). The third type is a dynamic system where dust-laden air is continuously introduced and exhausted from the chamber. Although using a whole-body exposure chamber is preferable and more comfortable for human subjects, there are some disadvantages of using such a system (Hammad & Pieretti, 2011). Exposing a subject's entire body to a given aerosol increases the chances that the material will be dermally absorbed or ingested instead of inhaled. Therefore it can be difficult to determine if a subject's health effects are due to inhalation of the material or ingestion/absorption. This type of chamber also leads to greater losses of the test material than head-only or nose-only inhalation systems, since each chamber run uses much more material than will be inhaled by a potential subject.

In a static or recirculating exposure chamber, the concentration is continuously decreasing.

However in a dynamic system, there is an initial rise in test material when the aerosol generator is first engaged before reaching a theoretical equilibrium (McClellan & Henderson, 1995).

Knowing the rate of this generation, the air flow rate, and the volume of the exposure system allows researchers to predict what the concentration (C) of the test material will be at equilibrium (Hammad & Pieretti, 2011). This is accomplished using Equation 1.

$$C = \frac{G}{Q} \quad \text{Equation 1}$$

Where,

C = concentration

G = generation rate of test material

Q = average flow rate of the exposure system

A unitless factor known as the “K” value, which ranges from 1 to 10, is often included in this equation to account for incomplete mixing (ACGIH, 2004). With the inclusion of the “K” value,

Equation 1 becomes:

$$C = \left(\frac{G}{Q} \right) K \quad \text{Equation 2}$$

Where a “K” value of 1 denotes complete, instantaneous mixing, with the other variables defined as they were in Equation 1.

In order to determine the concentration after a certain time has elapsed within the chamber (C_2), assuming initial concentration (C_1) is equal to 0, Equation 3 is used.

$$C_2 = \frac{KG \left[1 - e \left(- \frac{Q\Delta t}{KV} \right) \right]}{Q'} \quad \text{Equation 3}$$

Where,

Q' = effective ventilation (flow) rate

Δt = change in time

With all other variables as they were in Equations 1 and 2. In Equations 1 and 2, “Q” is the actual ventilation rate in Equation 3 whereas “Q'” is the effective ventilation (or flow) rate. This effective rate is calculated by dividing the actual ventilation rate by “K.” After aerosol

generation has ceased, the concentration within the exposure room will decrease over a period of time. This rate of decrease can be expressed as follows:

$$C_2 = C_1 e^{-\left[\frac{Q(t_2-t_1)}{KV}\right]} \quad \text{Equation 4}$$

Where, “C₁” is the concentration of the test material at the end of aerosol generation. With all other variables as they were in Equations 1, 2, and 3.

Literature Review

Health Effects of Air Pollution

Aerodynamic behavior of particles, subsequent deposition in the respiratory tract, and the effect on human health is largely determined by particle size. Deposition of particles in the respiratory system is often divided into three different fractions: inhalable, thoracic, and respirable (Hinds, 1999; Linnainmaa et al., 2007). Tables 1-3 display the collection efficiencies representative of the three mass fractions (ACGIH, 2015).

Table 1: ACGIH Inhalable Fraction

Particle Aerodynamic Diameter (μm)	Inhalable Particulate Matter (IPM) Fraction Collected (%)
0	100
1	97
2	94
5	87
10	77
20	65
30	58
40	54.5
50	52.5
100	50

Table 2: ACGIH Thoracic Fraction

Particle Aerodynamic Diameter (μm)	Thoracic Particulate Matter (TPM) Fraction Collected (%)
0	100
2	94
4	89
6	80.5
8	67
10	50
12	35
14	23
16	15
18	9.5
20	6
25	2

Table 3: ACGIH Respirable Fraction

Particle Aerodynamic Diameter (μm)	Respirable Particulate Matter (RPM) Fraction Collected (%)
0	100
1	97
2	91
3	74
4	50
5	30
6	17
7	9
8	5
10	1

An average adult inhales approximately 20 m³ of air each day (Curtis et al., 2006). With such a large volume of inhaled air, a slight change in outdoor air composition can have large health

effects. Categories of health effects from air pollution are often grouped based on the affected organ system: respiratory effects, cardiovascular effects, cancer, reproductive/developmental effects, mortality, infection, etc.

Curtis, et al. published a summary of recent research (from 1995 – 2005) on outdoor air pollution's many adverse health effects. They categorized human health effect data into eight major organ systems: respiratory, cardiovascular, cancer, reproductive and developmental, neurological, mortality, infection, and other. Respiratory effects comprise the majority of studies on outdoor air pollution. Examples of respiratory effects include asthma and COPD, especially in children and elderly populations, and several studies noted a correlation between increasing levels of outdoor particulate matter with a cut-point of 10 μm in aerodynamic diameter (thoracic fraction) and increased hospital admissions for these conditions (2006). There have also been studies that found a dose response relationship between thoracic fraction particle levels and bronchitis based on emergency room visits (Peel et al., 2005). Important contributors to outdoor air pollution respiratory health effects are traffic emissions, industrial pollution, mold/pollen/bioaerosols, biomass burning, and sand exposure (Delfino, 2002; From et al., 1992; Gyan et al., 2005; Koenig et al., 1997; Johnston et al., 2002; Larson et al., 1993; Koryeni-Both & Juncer, 1997; Lierl & Hornung, 2003; Targonski et al., 1995; Torigoe et al., 2000; Viswanathan et al., 2006).

Particle pollution, even at levels below the standards set by the Environmental Protection Agency (EPA) (listed below in Table 4), can also increase the risk of heart-related illness (EPA, 1990). Studies have found that even short term exposure to traffic pollution can trigger heart

attacks and that risk of cardiovascular disease from air pollution is particularly strong for women, diabetics and the elderly (Curtis et al., 2006).

Table 4: EPA National Ambient Air Quality Standards for Particle Pollution

Pollutant		Primary/Secondary	Averaging Time	Level
Particle Pollution Dec 14, 2012	PM _{2.5}	primary	Annual	12 µg/m ³
		secondary	Annual	15 µg/m ³
		primary and secondary	24-hour	35 µg/m ³
	PM ₁₀	primary and secondary	24-hour	150 µg/m ³

Studies conducted in Europe and the United States have found that individuals exposed to higher levels of outdoor PM_{2.5} and PM₁₀ are at a higher risk of developing lung cancer (Vineis et al., 2004). With regards to reproductive/developmental effects, a study conducted by Woodruff et al. on 4 million US infants found that increased levels of PM₁₀ were associated with increased death rates from sudden infant death syndrome (SIDS)(1997). Another study also found higher rates of preterm births in areas with increased PM₁₀ outdoor air levels (Sagiv et al., 2005).

Two large studies monitored the mortality/morbidity of 43 million European city dwellers and 50 million US city dwellers in response to the outdoor PM₁₀ concentration (Katsouyanni, Touloumi, & Samoli, 2001; Atkinson, Anderson, & Sunyer, 2001; Samet, Dominici, Curriero, Coursac, & Zeger, 2000; Zanobetti & Schwartz, 2005). The researchers found that each 10 µg/m³ increase of concentration of PM₁₀ resulted in the daily mortality increasing 0.6% in Europe and 0.5% in the US. This increase in PM₁₀ also produced statistically significant

increases in hospital admissions for COPD and heart disease (Katsouyanni et al., 2001; Atkinson et al., 2001; Samet et al., 2000; Zanobetti & Schwartz, 2005).

Curtis et al. concluded their review by praising the development of “environmental chambers to measure the respiratory effects of typical ambient levels of outdoor air pollution on humans (2006).”

Other Exposure Chamber Studies

A pioneering study using a whole body exposure chamber was conducted by Avol et al. in 1979. Epidemiologic studies before this point had linked sulfate aerosols to an increase in acute respiratory morbidity. However, these studies had been unsuccessful in identifying what specific pollutant was responsible for this increase. In Avol et al. study, human subjects were exposed to ammonium sulfate, ammonium bisulfate, and sulfuric acid at levels which would be considered “worst case” for the Los Angeles, California area (Avol et al., 1979). Subjects were exposed in groups to 100 $\mu\text{g}/\text{m}^3$ of ammonium sulfate, 85 $\mu\text{g}/\text{m}^3$ of ammonium bisulfate, and 75 $\mu\text{g}/\text{m}^3$ of sulfuric acid. The particle concentrations and size distributions were based on the highest value obtained from several 2-hour filter samples taken in the Los Angeles Basin. The subjects were required to perform baseline pulmonary function tests immediately upon entering the chamber, and then exercised on stationary bicycles for the first 15 minutes of every 30 minutes. The entire exposure lasted two hours.

The chamber used by Avol et al. was a dynamic system constructed from stainless steel, and it was continuously supplied with 14 m^3 of air each minute. A portion of this air was rerouted to a

mixing plenum, where it was combined with the agents before entering the chamber through a perforated ceiling. Uniform air distribution was accomplished by having an increased pressure in the air space above the perforated ceiling. Aerosol was generated using two banks of “Babington-type nebulizers” that were able to maintain mass concentrations between 10 to 1,000 $\mu\text{g}/\text{m}^3$. The aerosol concentration was monitored by an electrical aerosol analyzer and an optical particle counter. An air parcel was inside the chamber for an average of five minutes before being exhausted. Samples were also collected using a cascade impactor (Sierra Instruments 215S). The filter was removed immediately following sampling, and then underwent gravimetric and chemical analyses. Pulmonary function tests were performed after the 2-hour exposure to detect the presence of any short-term adverse effects. A one-way repeated-measures analysis of variance (ANOVA) was performed for the pulmonary function data to determine if there were differences among baseline measurements. Two-way repeated measures ANOVAs were done for the complete set of data. Results found little to no adverse health effects from the two hour chamber exposure (Avol et al., 1979). Repeatability was not addressed in this study.

Liden et al. designed a whole-body chamber for human dermal absorption and lung challenge tests (1998). They recognized the value of a chamber’s controlled environmental conditions for studying respiratory health effects. This is of particular importance when it comes to allergen studies, which have been known to have problems reproducing the same effect on subject after subject. Up to this point, environmental chambers mostly had been constructed to be used with gases only. It was possible to use the chamber in Liden et al.’s study, however, for both gases *and* particles, much like the chamber used in this study. Initial tests were performed with wheat flour, a well-known occupational allergen. The researchers chose stainless steel for constructing

the exposure chamber because it is inert to most experimental atmospheres, long-lasting, and will not build up an electrostatic charge. Three of the chamber's walls, the roof, and the floor were constructed of stainless steel while the front wall was built from glass in order to observe test subjects during experimentation and reduce subject discomfort. The chamber measured 1.8 m x 1.5 m x 2.1 m, for a total volume of 5.7 m³. This exposure room was connected to another space known as a "sluice" that measured 1.8 m x 0.9 m x 2.1 m that housed a hand shower and draining gutter. The hand shower was used to clean the exposure chamber in between experiments. The exposure chamber also contained ports that made it possible to connect sampling devices outside of the chamber to measure the concentration inside. These ports also could be used to supply fresh air for respiratory consumption, limiting allergen exposure to the skin only.

Air was taken from the room outside of the system and supplied to the exposure chamber with a centrifugal fan, after first being passed through Camfil Airopac CPM60 and CPM95 microfilters (Liden et al., 1998). The flow of air from the main air supply and secondary air supply produced an exchange rate of 6-12 air changes per hour in the chamber. The air then moved from the chamber to the sluice, where it was passed through another microfilter before being exhausted from the system. The exposure room was under higher pressure than the sluice (+2 Pa), which was under less pressure (- 1 Pa) than the outside air. This arrangement prevented the chamber from being contaminated from the sluice or outside air, and also prevented the sluice air from leaking into the outer room. The inclusion of a "forced exhaust" was a thoughtful addition on behalf of the researchers. This feature is installed in the air delivery system and can be activated

in cases where the exposure room air must be quickly evacuated. The researchers emphasized that all components in this air delivery system were easy to dismantle, replace, and clean.

A RBG 1000 aerosol generator was used since this device is preferred for aerosols, such as wheat flour, that cannot be easily packed (Liden et al., 1998). Dry powder is placed in a reservoir within the generator and a rotating brush above the reservoir coupled with a high-velocity air stream removes and blows the aerosol upwards. Liden et al. originally tried using a Wright Dust Feed for aerosol generation, but found that the device altered the wheat flour particle size distribution. They hypothesized that this was due to the packing and scraping required when using the Wright Dust Feed and switched to the RBG 1000 aerosol generator. As aerosol leaves the generator, it was passed through a neutralizer tube which contained a krypton 85 source. It was then mixed turbulently with clean air before entering downward into the exposure chamber. Mixing within the chamber was optimized by having a turbulent flow and by inserting a cone into the duct, forcing air to radially disperse. Spatial variability was measured by using multiple sampling devices in different locations within the chamber.

Total dust and respirable dust samples were conducted on 37 mm membrane filters. The Casella AMS950, a direct-read instrument, also was used to measure dust concentration (Liden et al., 1998). This instrument is based on infrared light scattering, and was calibrated against the total dust samplers. Personal Inhalable Dust Spectrometer (PIDS) cascade impactors were used to determine particle size distribution and the impactor plates were coated with 10% apiezone in toluene.

The concentration of wheat flour aerosol remained at a fairly constant 5 mg/m^3 for a two hour duration (Liden et al., 1998). It was determined that there was a greater percentage of inhalable particles in the chamber than in the real-world bakery environment. The researchers measured the temporal variation by calculating the coefficient of variation (CV) between readings taken every five minutes during one hour of exposure. This resulted in a CV range of 7-11% corresponding to a concentration of $4.2\text{-}5.1 \text{ mg/m}^3$. Spatial variation was calculated by running tests with and without human subjects, comparing the concentration results. No difference between spatial variation with and without a subject in the chamber was found. Particle size distribution results from the PIDS impactor indicated greater amounts of fine particles than commonly found in real-world bakery settings. However the researchers point out that this may become an advantage when performing future lung challenge studies since the potentially harmful fraction is increased.

In 2006, the same system was used to study temporal variations and spatial distribution within the chamber (Lundgren, 2006). A heated mannequin was also introduced in lieu of human subjects for these initial chamber studies. Several different agents were used: wheat flour, glove powder, cornstarch and pinewood dust. Temporal and spatial distributions were found to be less than 10% when close to the breathing zone and only slightly higher further away from the mannequin. The variability between each exposure session was also less than 10%. The aerodynamic particle size distribution curves were comparable to those found in occupational environments.

A study conducted by Lauralynn Taylor and her colleagues at The University of North Carolina (UNC) at Chapel Hill attempted to develop an exposure chamber for low-level concentration endotoxin exposures (2000). Goals of the study included construction of a chamber that allowed for thorough dust mixing, development of a dust generation system that was able to maintain concentrations at $250 \mu\text{g}/\text{m}^3$, and verification that the aerosol prepared for generation had a respirable size distribution and endotoxin concentration of 1300-1700 ng endotoxin/ ng dust. *Enterobacter agglomerans* was the origin of the endotoxin selected for the study, and this endotoxin was added as a coating onto cellulose dust.

The researchers constructed a 6.27 m^3 HEC as a partition off of an existing dust room at the UNC Chapel Hill Aerosol Laboratory. The chamber was constructed of sealed cinder block and Plexiglas, with glass windows to help prevent subject claustrophobia. Using an Aridata Multimeter Series 4800 (Shortridge Instrument Inc, Scottsdale, AZ), the researchers made sure that the chamber air exchange rate was at least 10 air exchanges per hour at all times. Air turbulence and uniform distribution were achieved using a fan. Air was exhausted to the outside atmosphere after being passed through a filter.

Cellulose was chosen as the carrier aerosol for the endotoxin because of its minimal health effects at low concentrations. The cellulose was heated to 100°C for one hour prior to sampling in order to verify that no additional endotoxins were present on the aerosol prior to the adhesion of *E. agglomerans* endotoxin. The endotoxin was added to the cellulose aerosol using an acetone absorption process. An aerosolized sample of the cellulose-endotoxin conglomerate was analyzed by light microscopy using a Porton graticule in order to confirm the respirable size

distribution of the material. Endotoxin content was confirmed using the Limulus Amebocyte Lysate (LAL) assay (Bio-Whittaker, Walkersville, MD).

Aerosol was dispersed using a dry aerosol generator in order to preserve the original particle size and endotoxin content. The dust feeder was a 6 cm diameter cylinder that was open at both ends, rotating freely on a 20.3 cm diameter rotating turntable. The turntable groove was uniformly filled with powder and dispersed using an aspirator.

The researchers cleaned the chamber between every run before re-coating the chamber walls with a thin layer of dust. Coating the chamber walls helped reduce the time for the dust concentration within the chamber to stabilize. This coating was developed by running the dust generator for approximately two hours. The researchers argue that without this “wall conditioning,” injected aerosol particles would be attracted to the chamber surfaces and not stay suspended within the chamber’s atmosphere.

Each chamber run was approximately four hours. Sampling equipment included three filters for total dust and a cascade impactor containing nine filters. A portable continuous aerosol monitor (PCAM) (Model 151, PPM Inc, Knoxville, TN) monitored the dust inside the chamber during each run. This instrument was able to provide real time measurements of dust concentration while the exposure was taking place. A modified method of the NIOSH 0500 method for total dust was used, collecting the samples at a flow rate of 10.5 L/min. The cascade impactor sampled at a flow rate of 6.8 L/min. The types of filters were also switched for each chamber run in order to determine which type of filter would be the most effective for endotoxin recovery.

Five filter types were used: gelatin, glass fiber, mixed cellulose ester, polyvinylchloride, and zeta. Filters that underwent gravimetric analysis were housed in a filter desiccator in order to control any potential moisture absorption.

The researchers achieved the three initial goals of the study:

- They were able to construct a HEC that had proper ventilation (11.5 air changes per hour), tolerated several washings, and was cost-effective.
- Dust was successfully generated and maintained at approximately $250 \mu\text{g}/\text{m}^3$. A one-factor ANOVA determined that the difference between the average dust concentrations of each chamber run was not statistically significant at a 95% confidence interval.
- The endotoxin concentration was within the respirable size range and was maintained between approximately 1300 and 1700 ng endotoxin/ mg dust.

Taylor et al. emphasized the need for continued studies on an exposure chamber before using it for human testing.

Suarez et al. set out to construct a single-pass, 10 m^3 stainless steel chamber in order to test the short-term effects of airborne contaminants (2005). The goal of this investigation was to develop a HEC that was somewhat inexpensive (~\$330,000) and simple to design and build, yet provided the proper facilities needed to do short-term aerosol testing. These criteria were satisfied by constructing the chamber as a single-pass system with no contact heating or cooling elements. The chamber could be operated in vapor-only mode or in a vapor + particulate mode, using environmental tobacco smoke (ETS). The respirable fraction of suspended particulate matter, which the researchers considered anything less than $10 \mu\text{m}$ in diameter, was measured using a

tapered element oscillating microbalance (TEOM). This article did a thorough job explaining the operating principles for vapor only and vapor + particulate exposure, as well as the development of an economical yet effective environmental chamber, but fell short when it came to thoroughly explaining the actual particulate measurement process and the instrumentation involved. They also failed to mention the spatial variability of the test material within the exposure chamber. During testing, the chamber was kept at 40% relative humidity (RH), 22.6°C, with an air flow rate of approximately 1055 liters/min. The aerosol was generated by having a human subject smoke a cigarette within the chamber. The researchers were aiming for a desired particle concentration of 100 $\mu\text{g}/\text{m}^3$ and were able to achieve this concentration 90% to 95% of the time during chamber runs. Also discussed was the inclusion of an antechamber, or mixing room, which they note will expand the range of challenge agents that can be studied with the chamber. This room was used to introduce the test material. With the antechamber, which was an additional 5 m^3 , the researchers were able to control the volume or mass of total vapor or particulate that entered the main chamber.

Eduard et al. discussed how beneficial an inhalation chamber can be to gain information on exposure-response relationships (2008). This type of information is usually obtained through epidemiological and animal studies. Their design criteria were very similar to the current project: they wanted to generate aerosols in the thoracic range with “a temporal and spatial variability of coefficient of variation < 10%.” They aimed for an exposure duration of two hours and concentrations of fused aluminum oxide particles of at least 4 mg/m^3 . The chamber used by the researchers was 16 m^3 and was constructed of acid-proof steel. The chamber has two glass doors and two windows constructed from polycarbonate. The tests were run at the lowest flow

rate to achieve a high concentration of the aerosol inside the chamber. The aerosol was generated using a fluidized bed generator, and the aerosol was then neutralized using a radioactive source. If the generator was operated with a cyclone, it was possible to adjust the particle size.

Once testing began, the researchers discovered a few problems with their design and experimental methods (Eduard et al., 2008). Dust started accumulating on the surface of the fluidized bed due to the shape of the flow obstructer beneath the bed plate. Tests were then done with different shaped flow obstructers until they reached a final design that gave the best mixing. They also encountered unexpected particle deposition in the upper section of the elutriator and in the inlet of the cyclone when concentrations greater than 1 mg/m^3 was reached. This deposition was reduced by applying vibration during the aerosol generation process using a pneumatic vibrator on the outside of the elutriator.

The experiment then progressed with human subjects in the chamber and a target concentration of 4 mg/m^3 (Eduard et al., 2008). They were able to reach the target concentration when the chamber was empty and also when the volunteer would enter the chamber and do two, 15-minute rounds of exercises on a stationary bike inside the chamber.

Results indicated that the particle mean diameter generated without the cyclone was $5.7 \text{ }\mu\text{m}$ and the particle mean diameter with a cyclone was $2.9 \text{ }\mu\text{m}$ (Eduard et al., 2008). The concentration of aerosols was 5.4% lower in the corners of the chamber than in the center and there were also statistically significant differences in other positions.

Prior research on the HEC used in this report was conducted by Hammad and Pieretti at the University of South Florida (2011). The first part of their research documents the performance of the chamber with gas phase agents. A separate report was prepared on the performance of the chamber with respirable particulate phase agents.

The researchers used CO₂ for evaluation of its performance, measuring the flow of gas entering the chamber with a dry-gas meter. Background CO₂ concentrations were measured before each chamber run and were accounted for during the generation measurements. A rotameter was also used to ensure that the flow rate of CO₂ into the chamber was consistent. Infrared instruments (Metrosonic aq-5000) were used to measure CO₂ levels. Buildup and decay patterns were measured in different areas of the exposure chamber. By examination of several consecutive patterns of buildup and decay for each chamber run, the researchers were able to predict the performance of the system. The CO₂ was generated at rates of 4.8, 8.5, and 11 L/min. The observed levels of CO₂ were very close to expected, and varied from the predicted concentrations by 0.62%-1.74%. These data support the conclusion that the exposure chamber system is reliable to use for inhalation challenge procedures for gases.

Other peer-reviewed articles concerning the performance and use of exposure chambers include those by Phalen (1976), Hammad et al. (1985), Rudell et al. (1996), Kimmel & Reboulet (1998), O'Shaughnessy et al. (2003), Gao et al. (2007), Wong (2007), and Shimada et al. (2009).

Experimental Methods

Chamber Specifications

The Plexiglas human exposure chamber was developed and used for studies using gases and/or particulates. It measures 4.16 ft x 2.67 ft x 6.75 ft, for a total volume of 75 ft³ or 2.13 m³.

Negative pressure operation at 4 inches of water ensures that contaminants do not leak into the room containing the chamber. The system can maintain a flow rate of approximately 34 cfm (1 m³/min).

Figure 1 depicts a schematic diagram of the chamber set up for particle generation, with the arrows representing the direction of air flow (Hammad & Pieretti, 2011). Room air is introduced through a HEPA filter and combines with dust-laden air in order to push the aerosol through the system and into the chamber. Air is exhausted through a HEPA filter. The filter is used to ensure that the air leaving the chamber does not contain any particulates used in the experiment. Particle monitoring devices are located within the chamber.

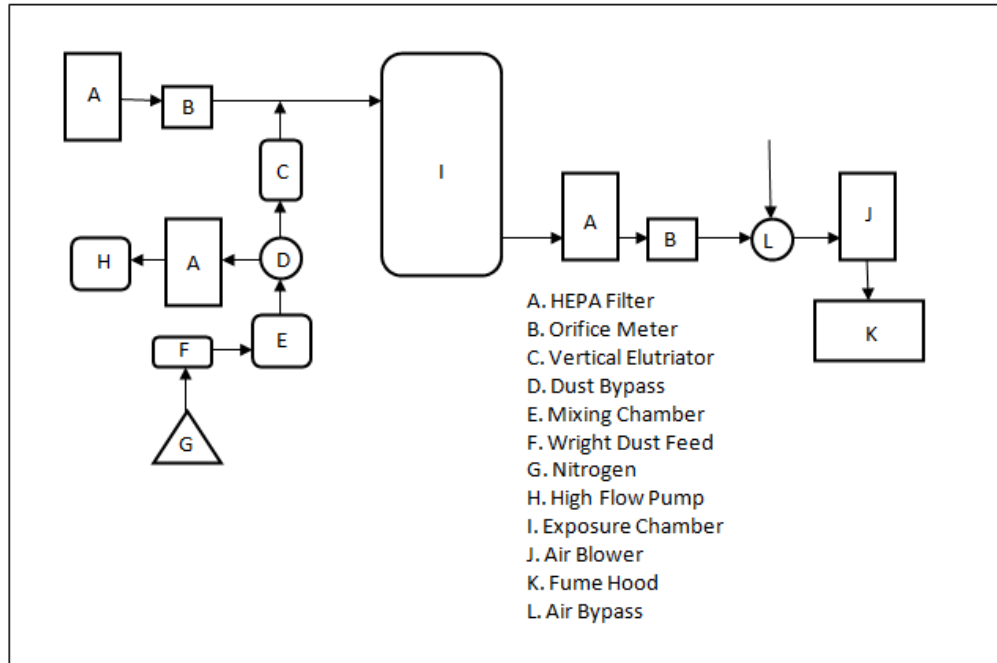


Figure 1: Diagram of Inhalation System

Exposure Chamber Components

A Spiral™ SL4P2 air blower is used to move air in the HEC. The blower is able to move a maximum of 2 m³/min. An air bypass is set up before the blower, and is used to control and regulate the flow rate of air into the chamber.

The measurement of air flow through the chamber is accomplished using orifice meters. Orifice meters are constructed using a one and a half inch diameter PVC duct and a plate. The plate has an orifice drilled into it that is one inch in diameter; air passes through this orifice and contracts the air flow. The point of contraction is known as the Vena Contracta. The orifice meters are connected to a Magnehelic gauge, which measures the pressure change before and at the Vena Contracta. This difference in pressure relates to the air flow rate. The orifice meters are

calibrated using a Micro-Pitot tube (Hinds, 1999) and a calibration curve was constructed for each orifice meter. One orifice meter was installed at the air intake (after a HEPA filter) and another was installed before the air blower.

Supply and exhaust air are filtered by High Efficiency Particulate Air (HEPA) filters. Three filters are used throughout the system. The first filter is positioned at the air intake of the HEC, which prevents particles from entering the system. The second HEPA filter is positioned after the chamber in order to collect aerosol before it enters the air blower. A third HEPA filter is used to collect the aerosol in the dust bypass.

Characteristics and Generation of Experimental Aerosol

The aerosol to be used in this research is a fine soda-lime glass particulate. (Baron, 1994). The typical composition of soda lime glass is silica (60-75%), soda (12-15%), and lime (5-12%). The addition of soda reduces the melting point of the glass, making the material more “manageable”, but less durable. This leads to the addition of the limestone, which increases the glass hardness and durability. The aerosol was purchased in narrow size categories from Fiber Optic Center, Incorporated (New Bedford, MA), and is spherical in shape. Figure 2 shows a photomicrograph of soda lime glass beads obtained by light microscopy.

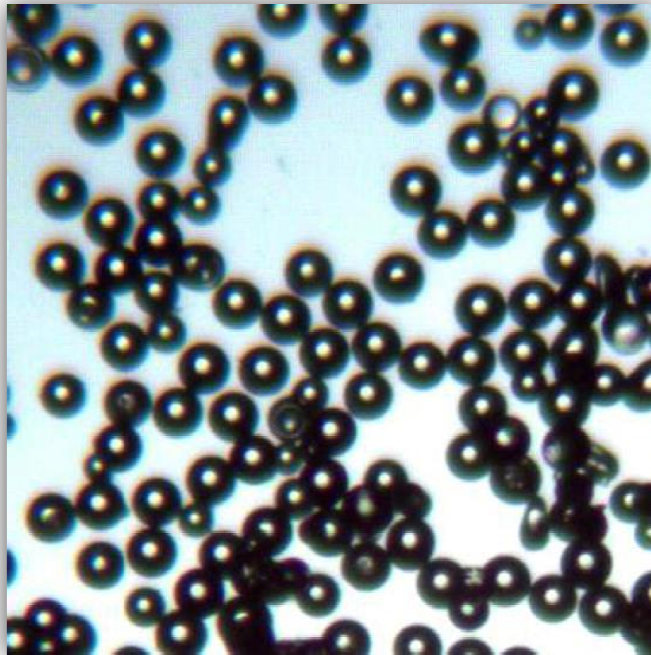


Figure 2: Photomicrograph of soda lime glass beads between 1 μm and 1 mm (2014)

The uniformity of shape and size, as well as dispersibility were the reasons for the selection of glass beads. Availability of an exposure chamber that is able to generate size-specific particulate would be beneficial for future studies assessing/evaluating human response to air pollution, which is normally in the thoracic fraction size range.

The glass beads can be dispersed as a dry powder using the Wright Dust Feed (WDF) (BGI Incorporated, Waltham, MA). Aerosol is packed into a cylinder using a two-ton Ann Arbor press for consistency, and a scraper blade in the cylinder slowly removes layers of the packed material, which is then transported into the test chamber by compressed nitrogen. The WDF has been used to generate several types of dust in previous investigations including silica, fly ash,

and abrasive blasting substitutes (Hammad et al., 1987; Abdel-Kader & Hammad, 1987). A diagram of the WDF is displayed in Figure 3.

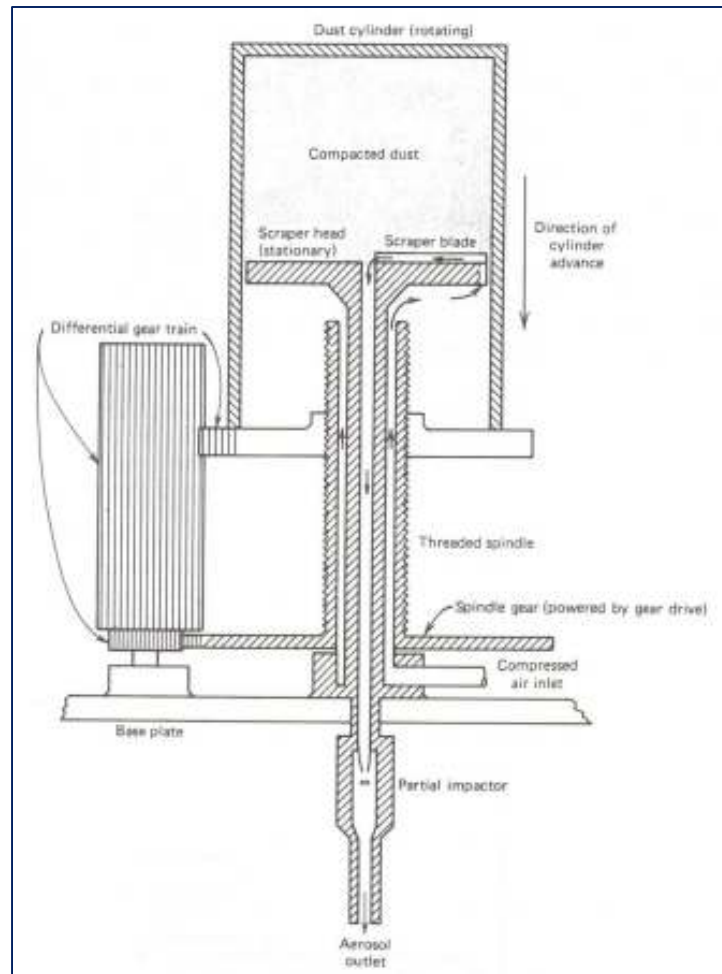


Figure 3: Diagram of Wright Dust Feed Mechanism (Hinds, 1999)

The aerosol is moved into the chamber by compressed nitrogen gas. The dust feeder can be set at various rotations per minute (RPM) settings in order to control the aerosol concentration entering the chamber. RPM settings used in this experiment were 0.4 and 0.8. The WDF was started 15 minutes before air enters the chamber, and a bypass was used during that time to

ensure that the aerosol is being generated evenly once it is allowed into the chamber. The glass beads are mixed with air in a dust mixing chamber (5 liter volume) constructed from PVC.

Aerosol Measurement

Monitoring devices usually used in an HEC include those which measure air flow, temperature, particle-size distribution, and concentration.

Before performing tests with a human exposure chamber, researchers need to ensure that the unit does not leak air in or out and is able to maintain a stable concentration. It is also important to know how much of the agent is expected to be lost between generation and delivery into the chamber and also if it is uniformly dispersed inside the chamber. The performance of the chamber used in this research has been previously tested and shown to have uniform dust and gas concentrations (Hammad & Pieretti, 2011). This consistency depends on the pattern of air flow through the chamber.

Aerosol concentration and consistency of its generation was determined using aerosol sampling cassettes. Particle concentration was determined by gravimetric methods, which are a common type of analysis for concentration when working with solid particles. Analysis was performed following the National Institute for Occupational Safety and Health's (NIOSH) Manual of Analytical Methods for Particulates Not Otherwise Regulated, Total Dust 0500. One of the limitations of using gravimetric analysis is that the concentration is not known until after the chamber run is complete. Therefore, aerosol concentration and particle size were also measured using two direct-read devices: a Tapered Element Oscillating Microbalance (TEOM) (Thermo

Fisher Scientific, Waltham, MA) and the QCM Cascade Impactor (California Measurements, Sierra Madre, CA).

The TEOM is a continuous sampler that consists of a substrate that is positioned on the end of a tapered, hollow tube (Baron, 1994). This tube is oscillated and particle-laden air is drawn through the filter before flowing through the tube. The frequency of the sampler decreases as particle accumulation increases. Measuring this frequency change provides an accumulated mass value. The TEOM displays a 10 minute average concentration (in $\mu\text{g}/\text{m}^3$), with an update every 2 seconds. With a TEOM sampler, possible gravimetric analysis errors such as filter handling are eliminated. The sampler is one of the most accurate direct-reading instruments for particulate mass in part due to its lower resonant frequency and vibrational motion that is parallel to the surface (Baron, 1994).

The 10-stage QCM Cascade Impactor (Model PC-2) has an aerodynamic diameter cut point range of 0.05 to 25 μm . The device is manufactured by California Measurements and operates at a 2 L/min flow rate. A printout of particle size distribution and mass concentration of ten size fractions is provided automatically after each sampling event.

Generation consistency was determined by conducting repeated chamber runs, documenting the concentrations and size-distribution. Using direct-read instruments provided better results with regards to the consistency of concentration of aerosol generation.

System Configurations

Several modifications were applied to the exposure chamber set up throughout this research, with a goal to generate particles in the thoracic-size range. Although the soda lime glass beads used for chamber runs were purchased in the several size ranges, the size of generated aerosol in the chamber in the initial stages was much smaller than the target size. The modifications to achieve the target size are divided into numerical steps so that they can be easily referenced and explained throughout this research. A minimum of three sampling runs were conducted for each modification before moving to another configuration.

Step 1: Removal of the vertical elutriator & elimination of 6 ft of PVC pipe

The vertical elutriator used in previous studies (See Figure 1) was removed from the set up in order to allow larger-size particles to enter the chamber. After several runs with this initial set up, the average particle diameter was still lower than desired. It was hypothesized that moving the aerosol generation closer to the chamber entry would increase particle size, since it would prevent larger particles from getting collected in the PVC pipe en route to the chamber.

Decreasing the travel distance for the aerosol would actually increase the amount actually getting in to the chamber. The pipe containing fresh filtered room air and dust-laden nitrogen gas was approximately 12 feet long from the generator to the ‘T’ section of PVC in Figure 4. The PVC pipe containing the aerosol was shortened by approximately 6 feet. The room air was introduced directly into the ‘T’ after traveling through the first orifice meter, as shown in Figure 4.

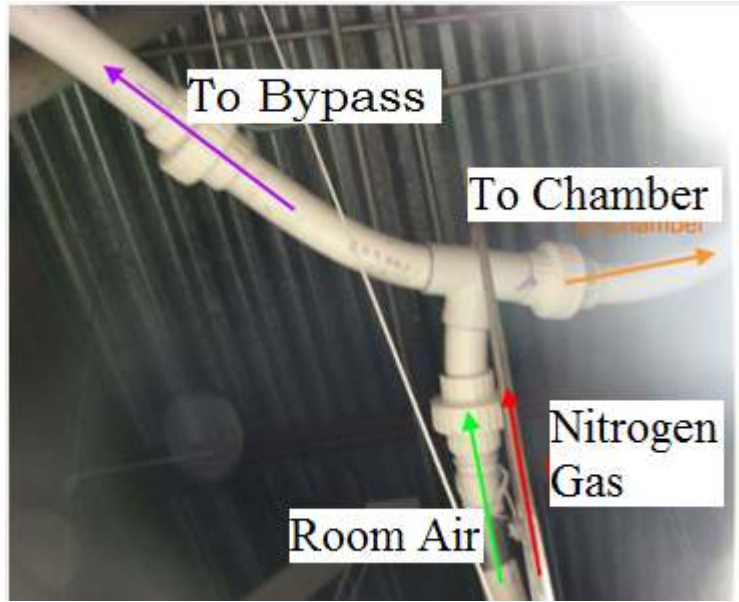


Figure 4: T-Shape Configuration

Step 2: Mixing chamber positioned horizontally

In the second configuration, the mixing chamber was positioned horizontally. Although the length of the piping had been reduced, the particle size reaching the chamber was still relatively smaller than expected.

Step 3: Placing mixing chamber directly over dust generator/RPM Reduction

The mixing chamber was moved closer to the aerosol generation in order to eliminate losses in the system. A new end cap was designed so that the dust-laden nitrogen entered at the bottom of the mixing chamber (Figures 5 and 6). A second hose nozzle was added to the bottom cap in order to connect another nitrogen tank and double the amount of gas entering the mixing chamber. It was hypothesized that with more gas pushing the aerosol upwards and towards the chamber, particles with a larger diameter would be carried more readily to the chamber. The RPM of the Wright Dust Feed was also reduced from 0.8 to 0.4 to decrease particle clumping/agglomeration encountered during aerosol generation.



Figure 5: New End Cap with Second Nozzle for Additional Nitrogen, Side View



Figure 6: New End Cap with Second Nozzle for Additional Nitrogen - Underside

Step 4: Additional clean air

A high flow pump with an air flow rate of 53 liters/min was attached to the bottom of the mixing chamber and the additional nitrogen was eliminated, in order to further promote the upward movement of the larger-size particles. The mixing chamber end cap was re-designed to have four small nozzles encircling a larger, central nozzle (Figures 7 and 8). The extra 53 L/min of clean air was distributed between the four perimeter nozzles, and the dust-laden nitrogen tubing from the generator was attached to the central nozzle.



Figure 7: End Cap Reconfigured with Four Perimeter Nozzles for Clean Air



Figure 8: End Cap Reconfigured with Four Perimeter Nozzles for Clean Air Inside View

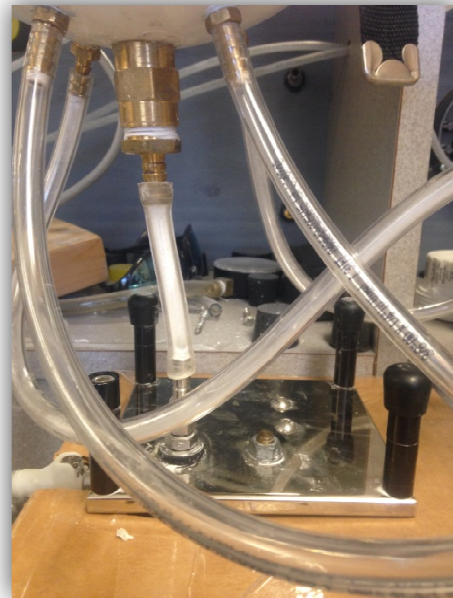
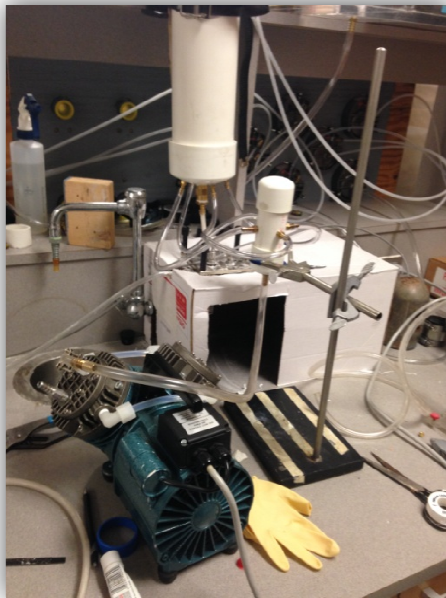


Figure 9: Shortened Tubing from Wright Dust Feed to End Cap

Step 5: Increasing glass beads to a nominal size of 7-15 μm

Larger size particles (7-15 μm batch) were used to increase the size of the particle generated in the chamber. Chamber runs were now conducted using the larger soda glass beads instead of the original 3-12 μm batch that was previously used.

A mannequin (Allen Display, Midlothian, VA) was also seated inside the chamber for several runs during this step to investigate its effect on the evenness of aerosol concentration and also to simulate the presence of a test subject in the chamber. A front and side view of the mannequin is displayed in Figure 10. The mannequin does not contribute to the efforts to increase particle size, therefore it was simply included in Step 5 and not given its own configuration step.

Mannequin measurement specifics are listed in Appendix D.



Figure 10: Mannequin Inside Chamber

Step 6: Slanted PVC configuration

The T-shaped junction where clean air was combined with the glass beads and entered the chamber was changed to a ‘Y’ configuration, as depicted in Figure 11. This change was made so that the aerosol would have a smoother path from the junction into the chamber, reducing wall loss on the PVC pipe due to impaction where the clean air meets the dust-laden air.

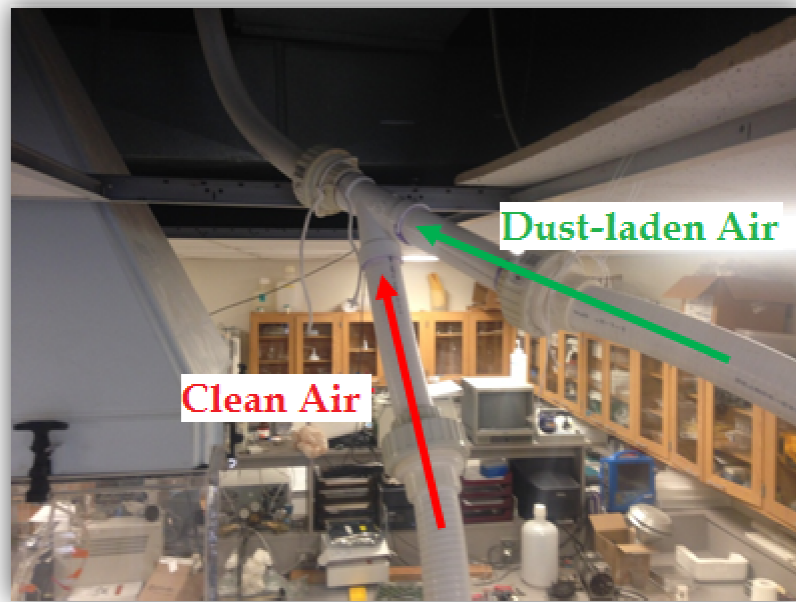


Figure 11: Slanted Junction Where Clean Air Meets Dust-Laden Air

Step 7: Elimination of Tygon tubing on WDF/Wider PVC opening

The Tygon tubing connecting the Wright Dust Feed to the bottom of the mixing chamber was eliminated in order to reduce particle loss along the sides of the tubing. The nozzle on the Wright Dust Feed was inserted directly into the bottom of the mixing chamber. The center nozzle inside the bottom of the end cap was enlarged in order to induce larger particulate to move upwards into the system. Figure 12 displays the wider PVC opening leading into the

mixing chamber. Figure 13 is an enlarged image depicting the WDF nozzle inserted directly into the bottom of the end cap through a rubber stopper.

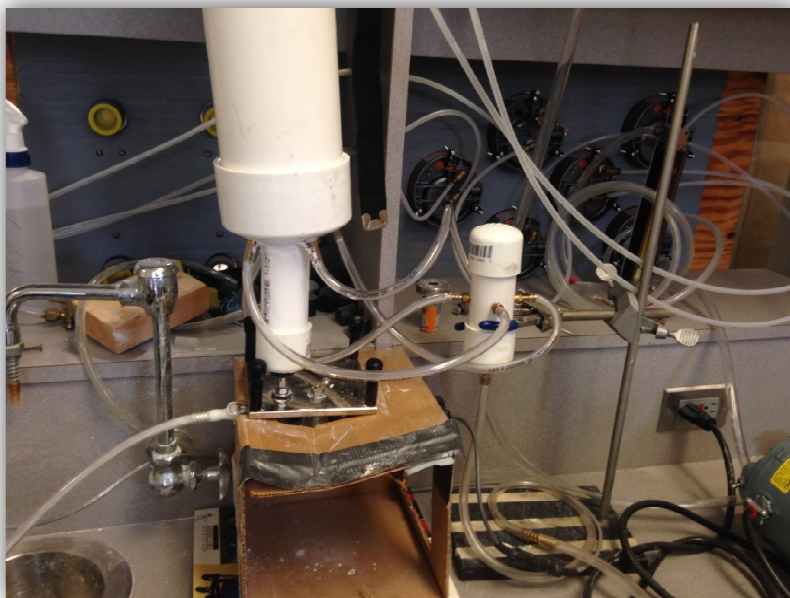


Figure 12: WDF Feeding Directly into End Cap



Figure 13: WDF Feeding Directly into End Cap - Enlarged Image

Step 8: Heated glass beads

To decrease possible particle agglomeration due to humidity, the glass beads were heated in an oven at approximately 125° C overnight before being packed into the Wright Dust Feed cylinder.

Step 9: Increasing glass beads to a nominal size of 25 µm

In the last step, a batch of glass beads with a 25 µm nominal size was used instead of the 7 – 15 µm beads used previously.

Analysis of Data

The average particle size distribution comparisons were performed using the geometric means of particle sizes obtained through the software program, DPlot (HydeSoft Computing, LLC, Vicksburg, MS). The Shapiro-Wilk test was used to confirm each configuration step's normality.

The Shapiro-Wilk test for normality was also used on the data representing evenness of concentration across the chamber. The sampling cassettes were divided into different groupings and compared using the student's t-test. The normality assumption was violated for one cassette group (Group D), so the Non parametric Wilcoxon Rank Sum test was used for all comparisons with this group.

Results and Discussion

Results have been categorized into two main sections. Section A displays data for the average particle size distribution for each configuration step of the chamber setup. Section B displays data for the evenness of concentration within the chamber.

The obtained data showed that the HEC dust generation system was capable of increasing the size of particulates on a consistent basis, and the thoracic size-fraction was produced. Spatial and temporal variability was minimal, as shown in the results below.

An average particle size distribution was determined for each reconfiguration step of the chamber setup. Each reconfiguration step followed a normal distribution based on the Shapiro-Wilk test for normality. The result was nine different averages, which were compared using the Welch-Satterthwaite t-test.

Section A: Particle Size Distributions

The purpose of this research was determining the average particle size at each configuration, in order to ultimately reach the thoracic size of 10 μm . All statistics and comparisons were performed using the geometric means of particle size obtained through the software program, DPlot (See Appendix F). Examination of Figure 14 indicates that each configuration increased

the mass median diameter (MMD) in the desired direction. Table 5 displays the mass median diameter in micrometers obtained at each configuration step, as well as a step description.

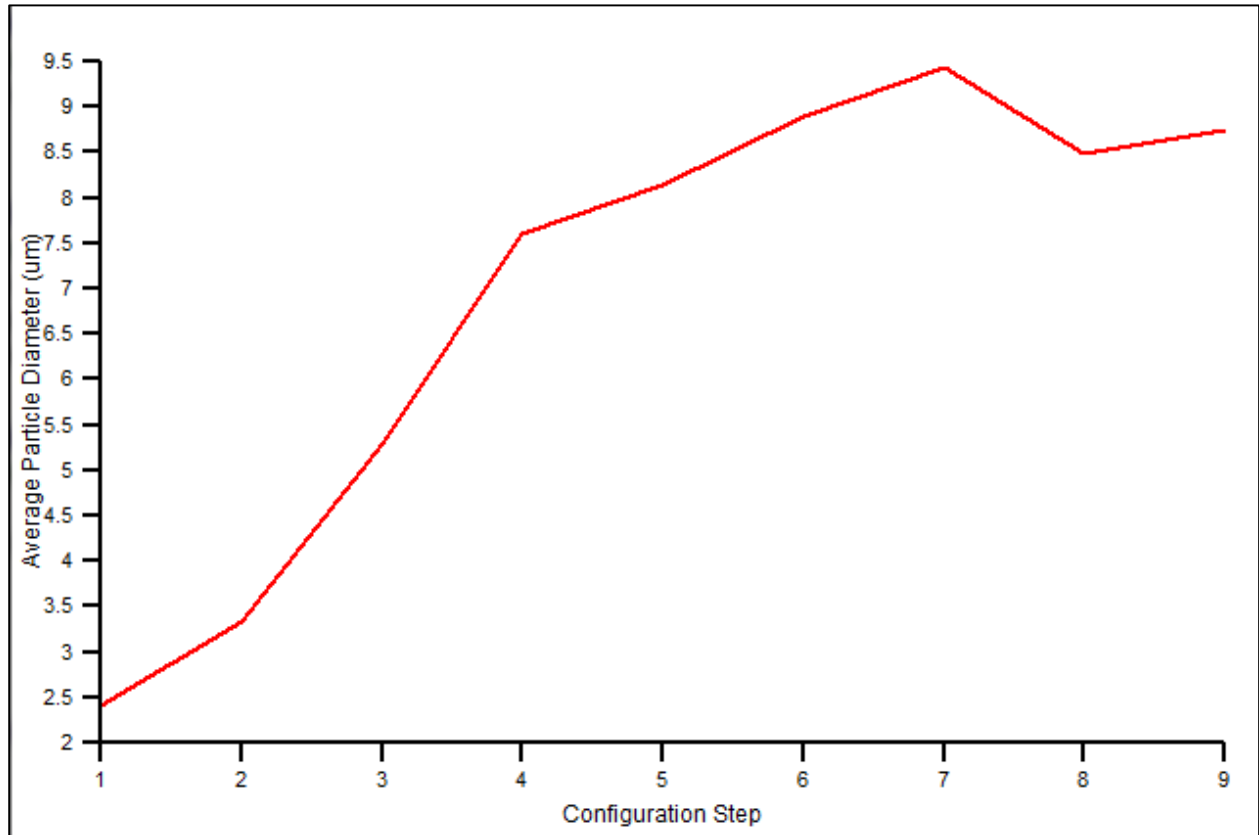


Figure 14: Average Particle Diameter Obtained for Each Step

Table 5: Mass Median Diameter (MMD) Obtained for each Chamber Configuration Step

Step	MMD (µm)	Step Description
1	2.42	removal of Vertical Elutriator
2	3.34	mixing chamber positioned horizontally
3	5.29	mixing chamber over top generator/rpm reduction
4	7.61	additional clean air (53 L/min)
5	8.14	larger (7-15 µm) dust
6	8.90	slanted PVC configuration
7	9.44	eliminated Tygon on WDF
8	8.48	heated glass beads
9	8.75	larger (25 µm) dust

The next measure was to calculate the statistical significance between each step. Each step was considered “normal” based on the Shapiro-Wilk test for normality, shown in Table 6, therefore parametric statistics were used.

Table 6: Tests for Normality for each Configuration Step

Step	Shapiro-Wilk Statistic (W)	Shapiro-Wilk p-value	Normal Based on Shapiro-Wilk?	Kolmogorov-Smirnov Statistic (D)	Kolmogorov-Smirnov p-value	Normal Based on Kolmogorov-Smirnov?
1	0.95	0.73	Yes	0.19	>0.15	Yes
2	0.82	0.12	Yes	0.25	>0.15	Yes
3	0.88	0.25	Yes	0.23	>0.15	Yes
4	0.82	0.05	Yes	0.32	0.02	NO
5	0.80	0.06	Yes	0.31	0.31	Yes
6	0.93	0.45	Yes	0.18	>0.15	Yes
7	0.95	0.58	Yes	0.27	>0.15	Yes
8	0.84	0.17	Yes	0.28	>0.15	Yes
9	1.00	1.00	Yes	0.26	>0.15	Yes

$\alpha = 0.05$

The null hypothesis was rejected because there were statistical differences between the size distributions obtained with certain configurations of the HEC. Table 7 displays the comparisons between each configuration step, and states if each comparison was statistically significant or not. Although the steps may appear correlated on first glance, they do not always have an intrinsic order (i.e.: step 1 does not cause step 2), therefore each reconfiguration step was treated as an independent sample and not correlated. T-tests were performed for each reconfiguration step comparison. In order to use a t-test, normality, independence, and homoscedasticity (equal variances) were assumed. There were two comparisons which were non-significant: step 6 to 7 and step 8 to 9. The most likely explanation for this non-significance is that the chamber system

was beginning to approach a ceiling limit of the size it was capable of producing. With the experimental set up it was not possible to increase the size beyond what has been obtained. The difference between step 5 and 6 (changing to a slanted PVC configuration) produced the smallest p-value and therefore could be thought of as the step having the most impact in terms of increasing the average particle diameter.

Table 7: Statistical Comparison Between Each Configuration – Independent Samples t-test

Step Comparison	p-value >	Statistically Significant?
1 and 2	0.004	Yes
2 and 3	0.006	Yes
3 and 4	0.004	Yes
4 and 5	0.016	Yes
5 and 6	0.001	Yes
6 and 7	0.342	No
7 and 8	0.035	Yes
8 and 9	0.780	No

Section B: Distribution of Concentration across the Exposure Chamber

Twelve total dust sampling cassettes were suspended from the ceiling of the HEC using Tygon tubing, 4.5 feet above the chamber floor. Figure 15 provides a plan view of the chamber displaying the cassette positions. The numbers in Figure 15 correspond to the sampler numbers themselves and have no further significance. The chamber was divided into different groups (A-E) in order to test for the evenness of concentration. These groupings are displayed in Figures 16 and 17.

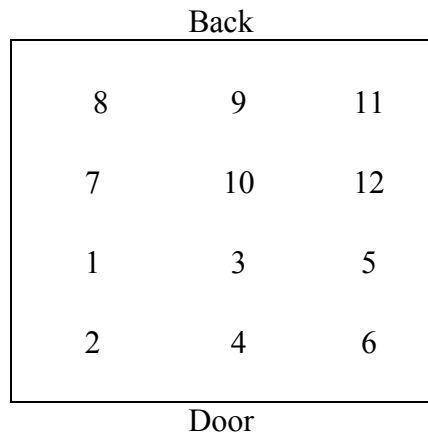


Figure 15: Plan view of Chamber with Numbered Cassette Locations

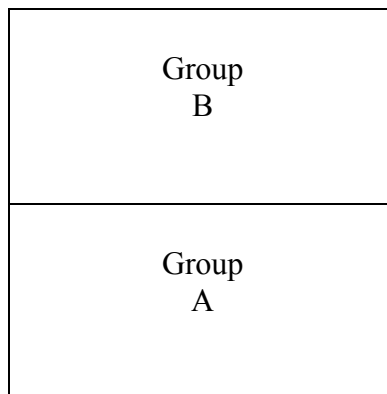


Figure 16: Plan View of Chamber Showing Groups A and B

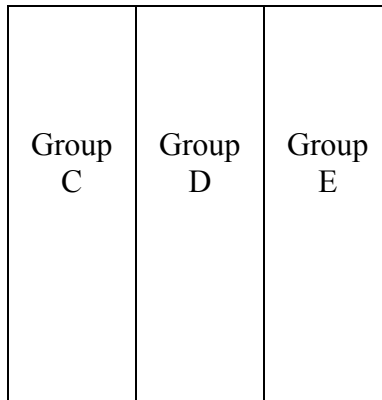


Figure 17: Plan View of Chamber Showing Groups C, D, and E

In order to make sure that there was not any one filter influencing the average concentration too far in either direction, the concentrations for each filter number were normalized to the mean and averaged over six runs. These normalized values are given in Table 8. This procedure was utilized to eliminate the effect of daily variability in aerosol concentration.

Table 8: Filter Concentrations Normalized to the Mean

Filter	Run 1 ($\mu\text{g}/\text{m}^3$)	Run 2 ($\mu\text{g}/\text{m}^3$)	Run 3 ($\mu\text{g}/\text{m}^3$)	Run 4 ($\mu\text{g}/\text{m}^3$)	Run 5 ($\mu\text{g}/\text{m}^3$)	Run 6 ($\mu\text{g}/\text{m}^3$)	Average Filter Conc
1	0.96	1.01	1.00	0.97	1.17	1.14	1.04
2	1.17	1.22	1.00	1.24	0.93	0.98	1.09
3	1.23	1.01	0.95	1.05	0.96	0.99	1.03
4	0.99	1.13	0.94	0.84	0.89	1.05	0.97
5	1.18	1.06	0.95	1.00	1.08	1.13	1.07
6	0.91	0.95	0.97	1.00	1.01	1.13	1.00
7	0.94	0.90	0.94	1.04	1.06	1.01	0.98
8	1.09	0.72	1.05	0.93	1.12	0.97	0.98
9	0.57	0.99	1.08	0.92	0.97	0.92	0.91
10	0.97	1.12	1.05	1.09	1.08	0.96	1.05
11	0.98	0.86	1.08	1.10	0.98	0.89	0.98
12	1.00	1.03	0.99	0.82	0.76	0.82	0.90
Avg	1.00	1.00	1.00	1.00	1.00	1.00	
SD	0.17	0.13	0.05	0.12	0.11	0.10	

The average filter concentrations from Table 8 were assigned to their respective cassette numbers in the plan view of the chamber (Figure 18). The plan view with the numbered cassette locations is also displayed for reference.

Back			Back		
0.98	0.91	0.98	8	9	11
0.98	1.05	0.90	7	10	12
1.04	1.03	1.07	1	3	5
1.09	0.97	1.00	2	4	6
Door			Door		

Figure 18: Chamber Diagram Showing Normalized Filter Concentrations

Table 9 displays the test for normality for the evenness of concentration data. The Shapiro-Wilk (SW) p-value was used instead of the Kolmogorov-Smirnov (KS) p-value because it performs better at a smaller sample size, and the KS statistic has less power and tends to get locked at a certain point.

Table 9: Test for Normality: Evenness of Concentration

Cassette Group	Sample Size (N)	Shapiro-Wilk Statistic (W)	Shapiro-Wilk p-value	Normal Based on Shapiro-Wilk?	Kolmogorov-Smirnov Statistic (D)	Kolmogorov-Smirnov p-value	Normal Based on Kolmogorov-Smirnov?
A	36	0.97	0.32	Yes	0.15	0.04	NO
B	36	0.97	0.49	Yes	0.08	>0.15	Yes
C	24	0.96	0.41	Yes	0.10	>0.15	Yes
D	24	0.91	0.04	NO	0.15	>0.15	Yes
E	24	0.97	0.73	Yes	0.11	>0.15	Yes

$\alpha = 0.05$

Although most of the comparisons between cassette groups within the chamber displayed in Table 10 had no statistically significant difference, the difference between Group A and B was slightly significant (p-value: 0.049, $\alpha = 0.05$). The difference is so small and cannot be readily explained, especially since it appeared only in this pattern of analysis. There may be slight variability between the A and B pattern as the dust is descending from the top of the chamber. All other comparisons, including individual comparisons of all twelve cassettes, were not statistically significant. The presence of a mannequin during Step 4 had no effect on the concentration distribution, based on a t-test comparison between data with and without the mannequin present. This is a favorable outcome when looking ahead to future work in the chamber with human subjects.

Table 10: Statistical Comparison of Open Face Cassette Patterns

Comparison	p-value >	Statistically Significant?
Group A and B	0.049	yes
Group C and D*	0.429	no
Group C and E	0.341	no
Group D* and E	0.916	no
All Cassettes	0.3941	no

$\alpha = 0.05$

*Non parametric Wilcoxon Ranks Sum test used due to violation of normality

Figure 19 depicts a Quantile plot for the Group A vs Group B sections of the chamber. Quantile plots provide a visual representation of the information previously given in Table 10. The figure has two data sets, depicting how closely those data sets follow a common distribution. In each graph there is a 45° reference line; data sets that come from populations with common distributions, and therefore are not statistically significant, will have points that fall closely to the reference line. If the points are farther away from the reference line, this would indicate that the two data sets are derived from populations with different distributions and may be statistically significant. (NIST/SEMATECH, 2012).

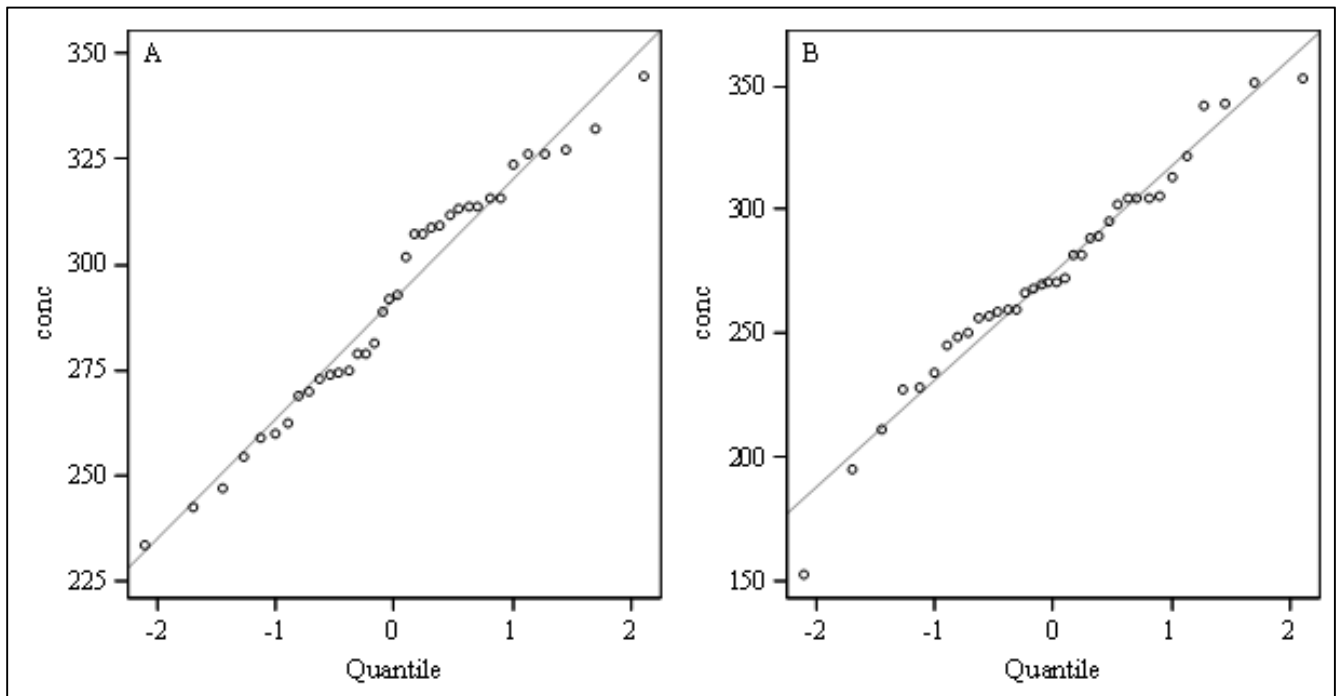


Figure 19: Comparison Quantile Plots for Groups A and B

Table 11 displays the average dust concentration for different chamber configurations as obtained by gravimetric analysis. The average concentration was not the best indicator of how well each chamber reconfiguration worked in getting towards the goal of a 10 μm average

particle size. As additional air was added, the average concentration would increase, most likely because more dust was being carried into the chamber due to the increased flow. However as larger dust sizes were used, the concentration fell again; it was speculated that the dust size became too large to be carried through the system and there was an increase in sedimentation and impaction. Tracking the concentration value was helpful during the runs themselves; using the real-time TEOM as the chamber was operating gave immediate feedback on how the chamber was functioning. A dramatic change in average concentration would indicate a failure within the system (i.e.: broken pump, blockage, generator malfunction, etc), and could be addressed immediately. The average dust concentration data for the TEOM is provided in Appendix H.

Table 11: Average Dust Concentrations Corresponding to Chamber Configurations, Obtained by Gravimetric Analysis

Step	Avg Conc ($\mu\text{g}/\text{m}^3$)	Step Description
1	285.48	removal of vertical elutriator & PVC elimination of 6 ft
2	221.79	mixing chamber on its side
3	424.60	mixing chamber over top generator/rpm reduction
4	1901.68	additional clean air (53 l/min)
5	2207.53	larger (7-15 μm) dust
6	1856.93	slanted PVC configuration
7	1568.10	eliminated Tygon on WDF
8	1472.23	baked beads overnight
9	803.85	larger (25 μm) dust

Conclusions

Research Hypotheses

For average particle size distribution at each reconfiguration step:

H₀: There is no statistical difference between the thoracic-fraction size distribution obtained with each configuration of the aerosol generation system.

H₁: There are statistical differences between the thoracic-fraction size distribution obtained with each configuration of the aerosol generation system.

For evenness of concentration across the chamber:

H₀: There is no statistical difference between total aerosol concentrations obtained by aerosol sampling for each cassette within the chamber.

H₁: There are statistical differences between total aerosol concentrations obtained by aerosol sampling for each cassette within the chamber.

Particle Size Distribution: Major Findings

The HEC is a useful tool for aerosol research, and can hopefully provide valuable data in future air pollution research as well. For the average particle size distribution at each reconfiguration step, the null hypothesis was rejected: particles approaching 10 µm can be successfully generated in the HEC. Statistically significant increases in size were observed in 7 of the 9 chamber reconfiguration steps. This indicates that the increasing size of particles entering the chamber was directly related to the different chamber configurations. It was important to introduce the changes to the chamber configuration in small increments to prevent the possibility of sudden change in particle size beyond 10 µm entering the chamber. The desired particle sizes in this

study are restricted to a certain size range of health significance, and larger particles are not of interest within the scope of this study.

Evenness of Concentration: Major Findings

With regards to the evenness of concentration within the chamber, the null hypothesis was upheld: other than a slightly borderline difference between Group A and B, there was no significantly statistical difference between the total dust concentrations obtained for each cassette within the chamber. Even when a mannequin was placed inside the chamber to simulate the presence of a human subject, there was no significant change in the evenness of concentration.

Study Strengths and Limitations

This research has helped to establish the USF Human Exposure Chamber's capability to produce particle sizes in the thoracic-range, and has also shown the system is proficient in producing an even concentration throughout the chamber interior. Incremental changes to the system's overall configuration were paramount in order to gradually approach the desired particle size without overshooting the mark, resulting in a strong correlation between configurations and increasing particle size. The research performed in this investigation can now be added to previous work that has shown the chamber's ability to produce particles in the respirable size range. Having an HEC able to consistently and evenly generate particles in both size ranges is very useful when marketing the system for future aerosol and air pollution studies.

The generated particle size plateaued at 10 μm , indicating that this is the maximum size to possibly achieve with the current experimental set up without a major re-engineering of the

chamber. Positioning the dust generator directly on the top of the chamber will reduce the travel path through PVC piping and eliminate possible bends in the piping system. Other future modifications could include using a different generation method. The main limitation of the HEC used in this research is that it is built to only contain one human subject, either sitting, standing, or riding an exercise bike.

Public Health Implications and Future Directions

Now more than ever, disease-prevention efforts are conducted on a global scale. Having a healthy outdoor environment is crucial to not only having a healthy workforce, but a healthy population as a whole. The WHO has reported that environmental factors are responsible for almost 25% of all deaths and the “total disease burden”. Many of the diseases which contribute the largest burden to this total, for instance lower respiratory infections, are also some of the most preventable. Lower respiratory infections can be attributed to environmental causes nearly 20% of the time in developed countries and 42% in developing nations. A 2008 EPA survey found that approximately 127 million people residing in the US lived in counties that exceeded at least one of the National Ambient Air Quality Standards (NAAQS). A human exposure chamber like the one used in this investigation is very valuable for conducting further research on particle pollution, which is an important NAAQS (EPA, 2008).

Exposure chambers can also be beneficial when conducting allergen exposure investigations and studies relating to allergies and asthma. A study recently published in September 2016 conducted field clinical trials of pollen allergy using a mobile human exposure chamber (Zuberbier et. al, 2016). Another study investigated the efficacy of an oral medication in treating house dust mite allergic rhinitis by using a human exposure chamber. Researchers determined

that using a HEC was useful in establishing a dose-dependent effect, and are planning on conducting further investigation of this problem (Roux et. al, 2016). Having a HEC whose performance capabilities have been well-established will allow for a broad range of public health research areas.

Typical outdoor air pollution can be categorized primarily as thoracic-size range. Having an HEC such as the one used in this investigation that can consistently generate particles in this size range allows for future air pollution studies. The chamber is large enough to fit a human subject, as well as an exercise bike to simulate work. Air pollution studies using human subjects within the chamber could provide valuable data on health-related issues associated with exposure to airborne particulates. This research has shown this chamber's utility in studying and assessing air quality. Future investigations can use this chamber to better understand individuals' responses to thoracic-sized particle pollutants, as well as the conditions in which people live and breathe.

References

- (2014). "Solid Soda Lime Glass Microspheres 2.5g/cc - Classified Grades 1um to 1mm." Retrieved September, 2014, from http://www.cospheric.com/SLGMSc_solid_glass_spheres_beads_microns.htm.
- Abdel-Kader HM, Hammad YY. (1987). "Distribution of Silica Dust Administered by Intratracheal Injection and Inhalation in Rat Lungs". Presented at the American Industrial Hygiene Conference, Montreal Canada.
- ACGIH (2004). Industrial Ventilation: A Manual of Recommended Practice. Cincinnati, ACGIH.
- ACGIH (2015). TLVs and BEIs. Signature Publications.
- Atkinson RW, Anderson HR, Sunyer J. (2001). "Acute effects of particulate air pollution on respiratory admissions: results from the APHEA2 study." Am J Respir Crit Care Med **164**:1860–6.
- Avol, E. L., M. P. Jones, et al. (1979). "Controlled Exposures of Human Volunteers to Sulfate Aerosols." American Review of Respiratory Disease **120**.
- Baron, P. A. (1994). "Direct-reading instruments for aerosols, a review.pdf". Analyst **119**(35-40).
- Curtis, L., W. Rea, et al. (2006). "Adverse health effects of outdoor air pollutants." Environment International **32**(6): 815-830.
- Delfino RJ, Zeiger RS, Seltzer JM, Street DH, Matteucci RM, Anderson PR, et al. (1997). "The effect of outdoor fungal spores concentrations on daily asthma severity." Environ Health Perspect **105**:622–35.
- Eduard, W., K. Kruse, et al. (2008). "Generation and Homogeneity of Aerosols in a Human Whole-Body Inhalation Chamber." Annals of Occupational Hygiene **52**(6): 545-554.
- EPA (1990). National Ambient Air Quality Standards. 40 CFR part 50.
- From LJ, Bergen LG, Humlie CJ. (1992). "The effects of open leaf burning on spirometric measurements in asthma." Chest **101**:1236–9.

- Gao, P., W. P. King, et al. (2007). "Review of Chamber Design Requirements for Testing of Personal Protective Clothing Ensembles." Journal of Occupational and Environmental Hygiene **4**(8): 562-571.
- Gyan K, Henry W, Lucille S, Laloo A, Lamsee-Ebanke C, McKay R, et al. (2005). "African dust clouds are associated with increased pediatric asthma accident and emergency admission on the Caribbean island of Trinidad." Int J Biometeorol **49**:371–6.
- Hammad YY, Abdel-Kader HM, Bozelka BE, Reynolds C, Strasma S, Que Hee SS. (1987). "Experimental Pneumoconiosis of Sandblasting Substitutes". Presented at the American Industrial Hygiene Conference, Montreal Canada.
- Hammad, Y. and Pieretti, L. (2011). "Performance of a human inhalation challenge exposure system. I. Gases." Inhalation Toxicology **23**(6): 331-338.
- Hammad YY, Rando RC, Abdel-Kader HM. (1985). "Considerations in the Design and Use of Human Inhalation Challenge Delivery Systems". Folia Allergologica et Immunologica Clinica **32**: 37-44.
- Hinds, W. C., Ed. (1999). Aerosol Technology: Properties, Behavior, and Measurement of Airborne Particles. New York, John Wiley & Sons, Inc.
- Jacobs J, Kreutzer R, Smith D. (1997). "Rice burning and asthma hospitalizations, Butte County, California, 1983–1992." Environ Health Perspect **105**:980–5.
- Johnston FH, Kavanagh AM, Bowman DM, Scott RK. (2002). Exposure to brushfire smoke and asthma: an ecological study." Med J Aust **176**:535–8.
- Katsouyanni K, Touloumi G, Samoli E. (2001). "Confounding and effect modification in the short-term effects of ambient particles on total mortality: results from 29 European cities within the APHEA2 project." Epidemiology **12**:521–31.
- Kimmel, E. C. and J. E. Reboulet (1998). "Calculation of exposure chamber leak rate with thermal correction - a measure of chamber integrity." American Industrial Hygiene Association Journal **59**: 779-784.
- Koenig JQ, Larson TV, Hanley QS, Reboliedo V, Dumler K, Checkoway H, et al. (1993). "Pulmonary function changes in children associated with exposure to particulate matter." Environ Res **63**:26–38.
- Korenyi-Both AL, Korenyi-Both AL, Juncer DJ. (1997). "Al Eskan disease: Persian Gulf Syndrome." Mil Med **162**:1-13.
- Liden, C., L. Lundgren, et al. (1998). "A New Whole-Body Exposure Chamber for Human Skin and Lung Challenge Experiments – The Generation of Wheat Flour Aerosols.pdf>." Annals of Occupational Hygiene **42**(8): 541-547.

- Lierl MB, Hornung RW. (2003). "Relationship of outdoor air quality to pediatric asthma exacerbations." Ann Allergy Asthma Immun **90**:28–33.
- Linnainmaa, M., J. Laitinen, et al. (2007). "Laboratory and Field Testing of Sampling Methods for Inhalable and Respirable Dust." Journal of Occupational and Environmental Hygiene **5**(1): 28-35.
- Lundgren, L. (2006). "Large Organic Aerosols in a Dynamic and Continuous Whole-Body Exposure Chamber Tested on Humans and on a Heated Mannequin." Annals of Occupational Hygiene **50**(7): 705-715.
- McClellan, R. O. and R. F. Henderson, Eds. (1995). Concepts in Inhalation Toxicology. Washington D.C., Taylor & Francis.
- Mercer, T. T. (1973). "Production and Characterization of Aerosols." Arch Intern Med **131**: 39-49.
- NIST/SEMATECH. (2012). "e-Handbook of Statistical Methods." <http://www.itl.nist.gov/div898/handbook/>, June 15, 2016.
- O'Shaughnessy, P. T., C. Achutan, et al. (2003). "A small whole-body chamber for laboratory use." Inhalation Toxicology **15**(3): 251-263.
- Peel J, Paige T, Klein M, Metzger KB, Flanders WD, Todd K, et al. (2005). "Ambient air pollution and respiratory emergency department visits." Epidemiology **16**:164–74.
- Phalen, R. F. (1976). "Inhalation exposure of animals.pdf>." Environmental Health Perspectives **16**: 17-24.
- Roux, , M., Devillier, P., Yang, WH., Montagut, A., Abiteboul, K., Viatte, A., Zeldin, RK. (2016). "Efficacy and safety of sublingual tablets of house dust mite allergen extracts: Results of a dose-ranging study in an environmental exposure chamber." J Allergy Clin Immunol **138**(2): 451-458.
- Rudell, B., M. C. Ledin, et al. (1996). "Effects on Symptoms and Lung Function in Humans Experimentally Exposed to Diesel Exhaust.pdf>." Occupational and Environmental Medicine **53**: 658-662.
- Samet JM, Dominici F, Curriero F, Coursac I, Zeger S. (2000). "Fine particulate air pollution and mortality in 20 US cities, 1987–1994." N Engl J Med **343**:1742–9.
- Sagiv SK, Mendola P, Loomis D, Herring AH, Neas LM, Savitz DA, et al. (2005). " A time-series analysis of air pollution and preterm birth in Pennsylvania, 1997–2001." Environ Health Perspect **113**: 602-6.

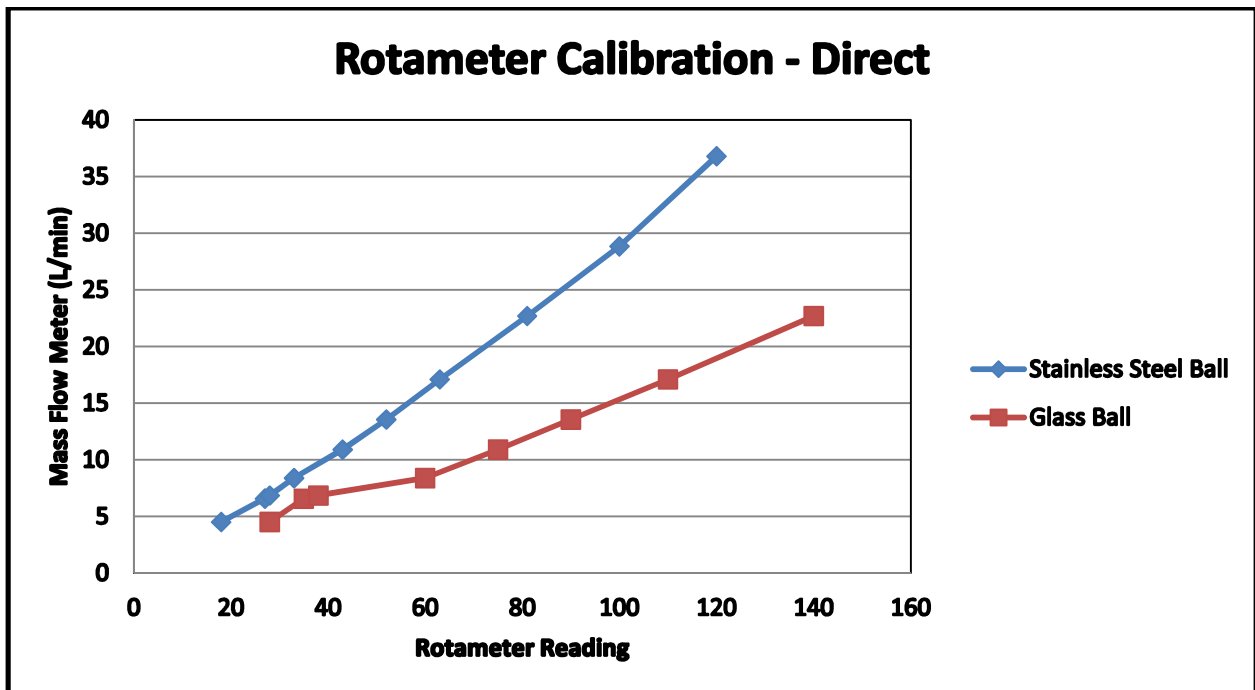
- Shimada, M., W.-N. Wang, et al. (2009). "Development and evaluation of an aerosol generation and supplying system for inhalation experiments of manuf nanoparticles.pdf>." Environmental Science & Technology **43**: 5529-5534.
- Suarez, J. C., D. S. Warmath, et al. (2005). "Single-Pass Environmental Chamber for Quantifying Human Responses to Airborne Chemicals." Inhalation Toxicology **17**(3): 169-175.
- Targonski P, Persky V, Ramakrishnan V.(1995). "Effect of environmental molds on risk of death from asthma during the pollen season." J Allergy Clin Immunol **95**:955–61.
- Taylor, L., P. C. Reist, et al. (2000). "Characterization of an Aerosol Chamber for Human Exposures to Endotoxin." Applied Occupational and Environmental Hygiene **15**(3): 303-312.
- Torigoe K, Hasegawa S, Numata O, Yazaki S, Magtsunaga M, Boku R, et al. (2000). "Influence of emission from rice straw burning on bronchial asthma in children." Pediatr Int **42**:143–50.
- US Environmental Protection Agency. (2008). "Our Nation's Air Status and Trends Through 2008." National Service Center for Environmental Publications. Research Triangle Park, NC: Office of Air Quality Planning and Standards.
- Vineis P, Foraster F, Hoek G, Lippsett M. (2004). "Outdoor air pollution and lung cancer: recent epidemiological evidence." Int J Cancer **111**:647–52.
- Viswanathan S, Eria L, Diunugala N, Johnson S, McClean C. (2006). "An analysis of effects of San Diego wildfire on ambient air quality." J Air Waste Manage Assoc **56**:56–67.
- Weyel, D., M. Ellakkani, et al. (1984). "An Aerosol Generator for the Resuspension of Cotton Dust." Toxicology and Applied Pharmacology **76**: 544-547.
- Wong, B. (2007). "Inhalation Exposure Systems: Design, Methods and Operation." Toxicologic Pathology **35**(1): 3-14.
- Woodruff TJ, Grillo J, Schoendorf KC. (1997). "The relationship between selected causes of postneonatal infant mortality and particulate air pollution in the US." Environ Health Perspect **105**:608–12.
- Zanobetti A, Schwartz J. (2005). "The effect of particulates on emergency admissions for myocardial infarction: a multicity case-crossover analysis." Environ Health Perspect **113**:978–82.

Zuberbier T, Abelson MB, Akdis CA, Bachert C, Berger U, Bindslev-Jensen C, Boelke G, Bousquet J, Canonica GW, Casale TB, Jutel M, Kowalski ML, Madonini E, Papadopoulos NG, Pfaar O, Sehlinger T, Bergmann KC; GALEN EU Network of Excellence in Allergy and Asthma. (2016). "Validation of the GA2LEN chamber for trials in allergy: Innovation of a mobile allergen exposure chamber." J Allergy Clin Immunol (Epub ahead of print).

Appendices

Appendix A: Rotameter Calibration

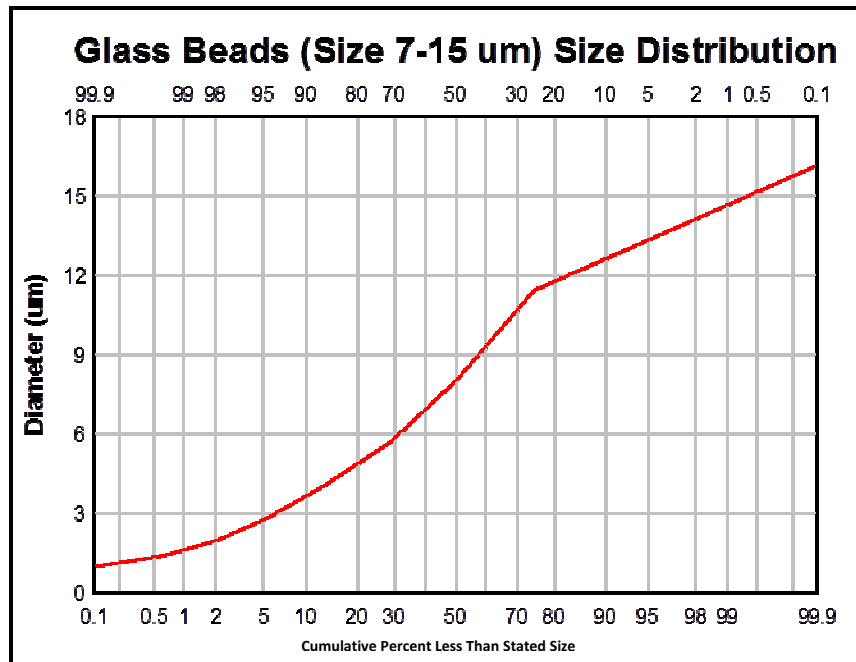
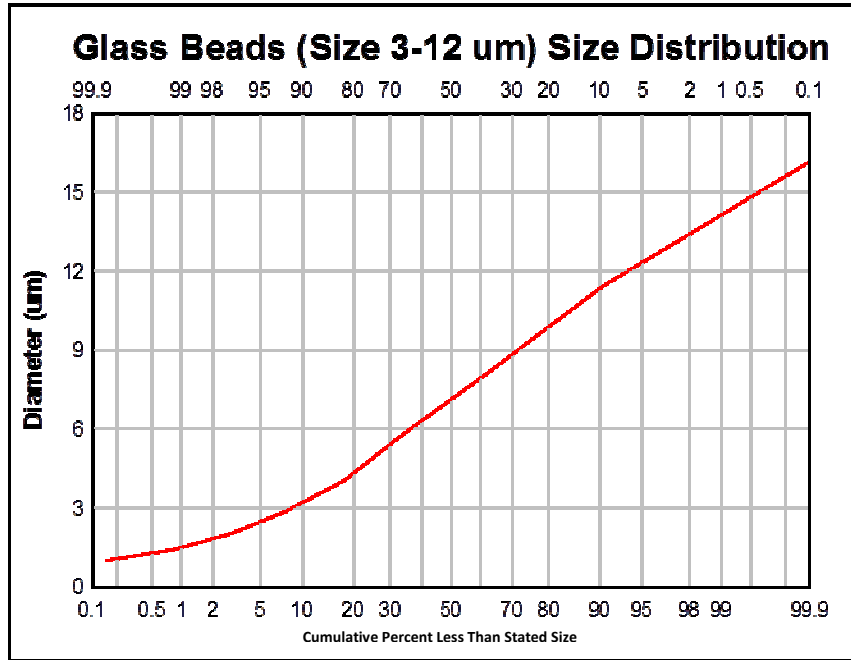
Glass Ball (Rot Reading)	St Steel (Rot Reading)	Mass Flow Meter (L/min)
28	18	4.51
35	27	6.57
38	28	6.85
60	33	8.39
75	43	10.9
90	52	13.55
110	63	17.1
140	81	22.69
	100	28.84
	120	36.79



Appendix B: Critical Orifice Calibrations

		Calibration #1	Calibration #2	Calibration #3	
Pump	Tube #	Avg of 5 Readings (L/min)	Avg of 5 Readings (L/min)	Avg of 5 Readings (L/min)	Standard Deviation
3/4 hp	1	3.337	3.343	3.364	0.0142
3/4 hp	2	2.958	2.891	3.369	0.2588
3/4 hp	3	3.338	3.349	3.376	0.0196
3/4 hp	4	3.951	3.966	4.000	0.0251
3/4 hp	5	3.932	3.926	3.968	0.0227
3/4 hp	6	3.938	3.947	3.985	0.0249
1/6 hp	7	2.749	2.747	2.762	0.0081
1/6 hp	8	2.775	2.772	2.766	0.0046
1/6 hp	9	2.685	2.718	2.713	0.0178
1/6 hp	10	2.691	2.718	2.669	0.0245
1/6 hp	11	2.673	2.67	2.656	0.0091
1/6 hp	12	2.715	2.713	2.698	0.0093

Appendix C: Determination of Size Distribution of Glass Beads by Light Microscopy



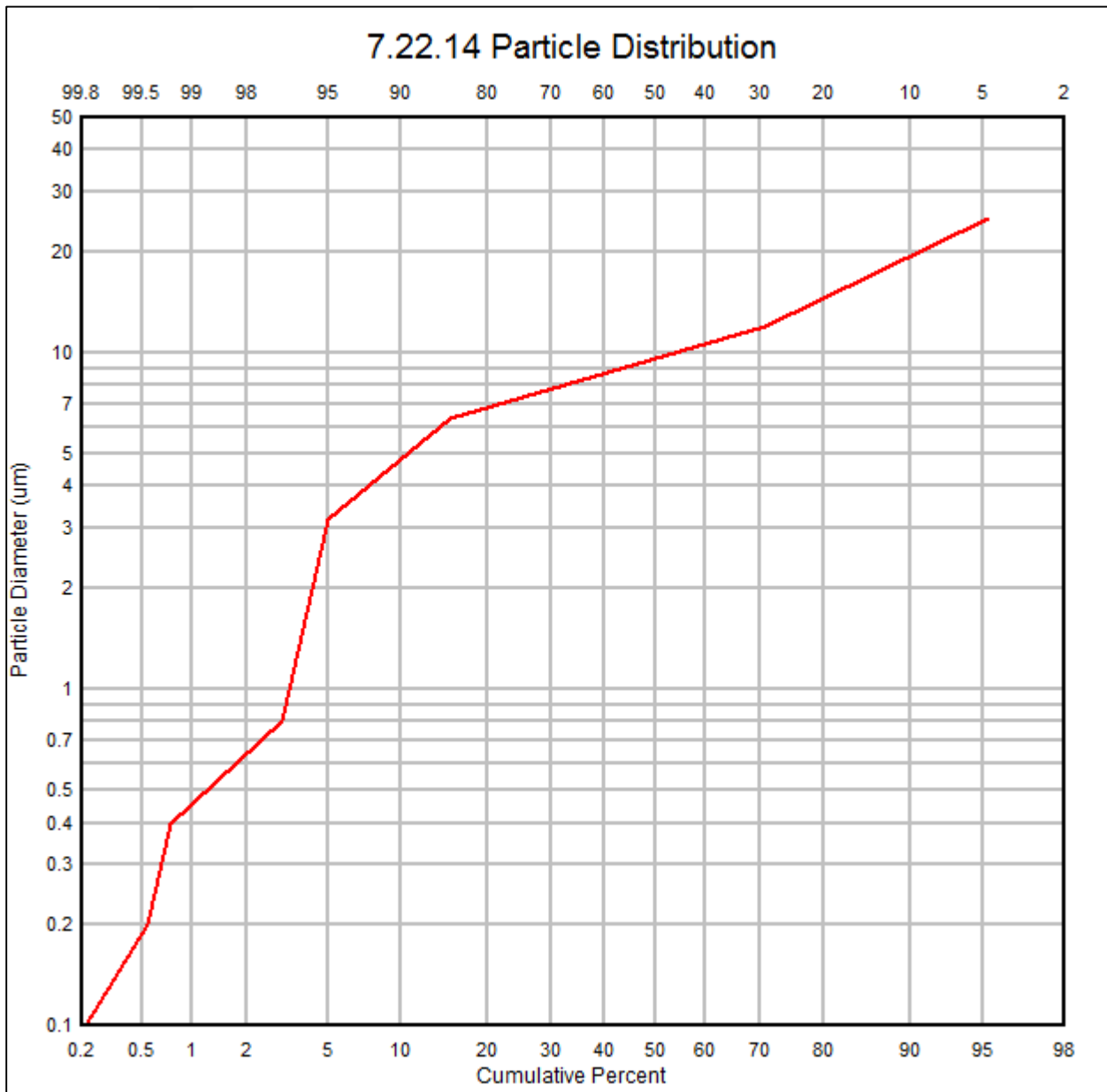
Appendix D: Mannequin Measurements

Height	73 1/2"
Neck	13 1/2"
Shoulders	18 1/2"
Chest	39 1/4"
Bicep	13 5/8"
Waist	30 1/2"
Hip	39 1/2"
Thigh	21 1/2"
Calf	16 1/4"
Inseam	34"
Sleeve	35"
Outside Foot Measurement	15 1/5"
Foot Style	Abstract

Appendix E: Particle Size Distribution for Each Reconfiguration Step

Step 1	GM (µm)	2.00	2.10	2.40	2.40	2.70	2.90					
	GSD	2.19	2.26	2.17	2.33	1.88	2.43					
Step 2	GM (µm)	2.74	3.00	3.00	3.07	3.20						
	GSD	1.97	1.77	1.90	1.98	1.83						
Step 3	GM (µm)	4.17	4.58	4.7	7.4	5.29	5.6					
	GSD	1.89	1.85	2.01	1.99	1.67	1.57					
Step 4	GM (µm)	7.56	6.86	7.58	7.74	7.67	7.61	7.8	8.01			
	GSD	1.34	1.63	1.36	1.48	1.39	1.40	1.47	1.48			
Step 5	GM (µm)	8.41	7.66	7.66	8.31	8.50	8.27	7.84	7.85	8.36	8.43	8.10
	GSD	1.39	1.42	1.42	1.51	1.48	1.45	1.38	1.45	1.50	1.42	1.41
Step 6	GM (µm)	9.53	8.87	8.70	9.13	8.68	8.91	8.49	8.76	8.78	9.11	
	GSD	2.16	1.55	1.48	1.57	1.49	1.60	1.41	1.47	1.48	1.54	
Step 7	GM (µm)	8.60	10.08	9.63								
	GSD	1.51	1.54	1.67								
Step 8	GM (µm)	8.27	8.15	8.70	8.60	8.68						
	GSD	1.41	1.49	1.45	1.44	1.38						
Step 9	GM (µm)	9.5	8									
	GSD	1.55	2.46									

Appendix F: An Example of a DPlot graph as Determined by Impactor



Appendix G: MSDS for Soda Lime Glass Beads



1. MATERIAL IDENTIFICATION

Product Name: **ANGSTRÖMSPHERE Soda Lime Beads**

Emergency Phone: For product emergencies involving spill, leak, fire, exposure, or accident call CHEMTREC at (800) 424-9300. For all other inquiries call **Fiber Optic Center™, Inc.** at (800) 473-4237.

2. COMPOSITION

Hazardous Components	CAS No.	Percent	Exposure Limits	
			ACGIH TLV-TWA	OSHA PEL
Glass, oxide; Glass	65997-17-3	100%	15 mg/m ³ total dust 5 mg/m ³ respirable	10 mg/m ³ Inhalable 3 mg/m ³ respirable

3. HEALTH HAZARDS IDENTIFICATION

Primary Routes of Exposure: Eyes: Yes Skin: Yes Inhalation: Yes

Eye Contact: Practically not irritating to the eyes

Skin Contact: Slightly irritating to the skin

Inhalation: No known hazards

Ingestion: No Known hazards

4. FIRST AID MEASURES

Eyes: Flush eyes with plenty of water for at least 15 minutes. Seek medical attention if discomfort persists.

Skin: Wash with plenty of water. Remove contaminated clothing and shoes. Seek medical attention if irritation develops or persists.

Inhalation: None required

Ingestion: None required

5. ACCIDENTAL RELEASE MEASURES

Personal protection: Wear eye goggles. Wear rubber boots with slip-resistant soles, and NIOSH-approved dust respirator where dust occurs.

Environmental Hazards: Sinks in water. No known hazard to aquatic life

Small Spills: Carefully shovel or sweep up spilled material and place in suitable container. Avoid generating dust

Large Spills: Keep unnecessary people away; isolate hazard area and deny entry. Do not walk through spilled material. Carefully shovel or sweep unspilled material and place in a suitable container. Avoid generating dust.

Disposal Considerations: Dispose in accordance with federal law.

Storage: Keep containers closed. Store in metal, fiber or glass containers.

ANGSTRÖMSPHERE™ is a trademark of Fiber Optic Center, Inc., New Bedford MA, USA

Fiber Optic Center™, Inc. MAKES NO EXPRESS OR IMPLIED WARRANTIES OF MERCHANTABILITY, FITNESS OR OTHERWISE, with respect to its products. In addition, while the information herein is believed to be reliable, no warranty is expressed or implied regarding the accuracy of the data or the results to be obtained from the use thereof. All recommendations or suggestion for use are made without guarantee – inasmuch as conditions of use are beyond our control. The properties given are typical values, and are not intended for use in preparing specifications. Users should make their own test to determine the suitability of this product for their own purposes.

Rev. A 04/2010
Fiber Optic Center™, Inc., 23 Centre Street, New Bedford, MA, 02740-6322, USA E-mail: sales@focenter.com
 Toll Free: (800) IS-FIBER or (800) 473-4237 • Phone: (508) 992-6464 • Fax: (508) 991-8876 • Website: www.focenter.com

Appendix H: TEOM Data vs Gravimetric Data for Average Particle Concentration

The TEOM is a real-time sampling instrument that was used during each chamber run in this research. The average particle concentration was obtained through the TEOM and also through gravimetric analysis of total dust cassettes (NIOSH Manual of Analytical Methods – Particulates Not Otherwise Regulated, Total 0500). The average particle concentrations were not of primary importance for the purposes of this investigation, but have been listed in the table below for reference.

Step	Avg Conc TEOM ($\mu\text{g}/\text{m}^3$)	Avg Conc Gravimetric ($\mu\text{g}/\text{m}^3$)
1	250.25	285.48
2	212.44	221.79
3	290.40	424.6
4	1668.42	1901.68
5	2384.05	2207.53
6	1944.50	1856.93
7	1538.11	1568.1
8	1287.57	1472.23

Appendix I: Copyright Clearance - John Wiley & Sons

JOHN WILEY AND SONS LICENSE TERMS AND CONDITIONS

Nov 30, 2016

This Agreement between Laura F Riley ("You") and John Wiley and Sons ("John Wiley and Sons") consists of your license details and the terms and conditions provided by John Wiley and Sons and Copyright Clearance Center.

License Number	3999050725935
License date	Nov 30, 2016
Licensed Content Publisher	John Wiley and Sons
Licensed Content Publication	Wiley Books
Licensed Content Title	Aerosol Technology: Properties, Behavior, and Measurement of Airborne Particles, 2nd Edition
Licensed Content Author	William C. Hinds
Licensed Content Date	Jan 1, 1999
Licensed Content Pages	504
Type of use	Dissertation/Thesis
Requestor type	University/Academic
Format	Print and electronic
Portion	Figure/table
Number of figures/tables	1
Original Wiley figure/table number(s)	Figure 21.4
Will you be translating?	No
Title of your thesis / dissertation	Expansion of the Performance Capabilities of the USF Inhalation Challenge Chamber
Expected completion date	Dec 2016
Expected size (number of pages)	75